Katholieke Universiteit Leuven

Departement Elektrotechniek ESAT-SISTA/TR 07-30

Adaptive Feedback Cancellation for Audio Applications[1]

Toon van Waterschoot[2] [3] and Marc Moonen[2]

October 2008
Published in *Signal Processing*, vol. 89, no. 11, Nov. 2009, pp. 2185-2201.

[1]This report is available by anonymous ftp from *ftp.esat.kuleuven.be* in the directory *pub/sista/vanwaterschoot/reports/07-30.pdf*

[2]K.U.Leuven, Dept. of Electrical Engineering (ESAT), Research group SCD(SISTA), Kasteelpark Arenberg 10, B-3001 Leuven, Belgium, Tel. +32 16 321927, Fax +32 16 321970, WWW: *http://www.esat.kuleuven.be/sista-cosic-docarch*. E-mail: *toon.vanwaterschoot@esat.kuleuven.be*.

[3]This research work was carried out at the ESAT laboratory of the Katholieke Universiteit Leuven, in the frame of K.U.Leuven Research Council: CoE EF/05/006 Optimization in Engineering (OPTEC) and the Belgian Programme on Interuniversity Attraction Poles, initiated by the Belgian Federal Science Policy Office IUAP P6/04 (DYSCO, 'Dynamical systems, control and optimization', 2007-2011), and the Concerted Research Action GOA-AMBioRICS, and was supported by the Institute for the Promotion of Innovation through Science and Technology in Flanders (IWT-Vlaanderen). The scientific responsibility is assumed by its authors.

Signal Processing 89 (2009) 2185–2201

Contents lists available at ScienceDirect

Signal Processing

journal homepage: www.elsevier.com/locate/sigpro

Adaptive feedback cancellation for audio applications

Toon van Waterschoot *, Marc Moonen

Katholieke Universiteit Leuven, ESAT-SCD, Kasteelpark Arenberg 10, B-3001 Leuven, Belgium

ARTICLE INFO

Article history:
Received 31 December 2008
Received in revised form
14 April 2009
Accepted 29 April 2009
Available online 8 May 2009

Keywords:
Acoustic feedback
Adaptive feedback cancellation
Audio signals
Public address
Hearing aids

ABSTRACT

Acoustic feedback occurs in many audio applications involving musical sound signals. However, research efforts in acoustic feedback control have mainly been focused on speech applications. Since sound quality is of prime importance in audio applications, a proactive approach to acoustic feedback control is preferred to avoid ringing, howling, and excessive reverberation. Adaptive feedback cancellation (AFC) using a prediction-error-method (PEM)-based approach is a promising proactive solution, but existing algorithms are again designed for speech applications only. We propose to replace the all-pole near-end speech signal model in the PEM-based approach with a cascade of two near-end signal models: a tonal components model and a noise components model. We derive the identifiability conditions for joint identification of the acoustic feedback path and the cascaded near-end signal models. Depending on the model structure that is used for the near-end tonal components, three different PEM-based AFC algorithms are considered. By applying some relevant model approximations, the computational overhead of the proposed algorithms compared to the normalized least mean squares (NLMS) algorithm can be reduced to 25% of the NLMS complexity. Simulation results for both room acoustic and hearing aid scenarios indicate a significant performance improvement in terms of the misadjustment and the maximum stable gain increase.

© 2009 Elsevier B.V. All rights reserved.

1. Introduction

Acoustic feedback is a physical phenomenon arising in several speech and audio applications, which may severely degrade sound quality and may even cause damage to human hearing and to loudspeaker components. When a sound signal is picked up by a microphone and then amplified and played back in the same acoustic environment, a closed signal loop is created, which may give rise to system instability. The existence of an acoustic feedback path limits a sound system's performance in two ways. First of all, there is an upper limit to the amount of amplification that can be applied if the system is required to remain stable, which is referred to as the maximum stable gain (MSG). Second, the sound quality is affected by occasional howling when the MSG is exceeded, or, even when the system is operating below the MSG, by ringing and excessive reverberation.

Many solutions to the acoustic feedback problem have been proposed, see van Waterschoot and Moonen [1] for an overview and a comparative evaluation of state-of-the-art methods. Apart from manual feedback control, the two most promising solutions are notch-filter-based howling suppression (NHS) [2–5] and adaptive feedback cancellation (AFC) [6–23]. Research efforts in acoustic feedback control so far have mainly dealt with speech applications. In this paper, we explicitly focus on feedback control in audio applications involving musical signals, e.g., public address (PA) systems in concert venues, or hearing aids (HA) operating in a musical environment. When dealing with audio instead of speech applications, two major issues should be taken into account. First of all, whereas in

* Corresponding author. Tel.: +32 16 321927; fax: +32 16 321970.
E-mail addresses: toon.vanwaterschoot@esat.kuleuven.be (T. van Waterschoot), marc.moonen@esat.kuleuven.be (M. Moonen).
URL: http://homes.esat.kuleuven.be/~tvanwate (T. van Waterschoot).

0165-1684/$ - see front matter © 2009 Elsevier B.V. All rights reserved.
doi:10.1016/j.sigpro.2009.04.036

speech applications intelligibility is of prime interest, for audio applications sound quality becomes much more important. Second, audio signals typically exhibit a much higher degree of tonality than speech signals, whereas many feedback control methods are not designed to work with tonal signals. In fact, none of the state-of-the-art solutions is capable of meeting these two requirements [1]. From a sound quality point of view, the NHS approach is inappropriate due to its reactive nature, i.e., howling, ringing, and excessive reverberation cannot be avoided. Moreover, in the NHS howling detection, discriminating between undesired feedback oscillations and desired tonal components in the microphone signal spectrum is a non-trivial task [1,2,4,5]. Existing AFC techniques are generally also not appropriate for audio applications. Due to the AFC signal correlation problem, the use of a decorrelation method is required to avoid the adaptive filter from converging to a biased feedback path estimate [1,12,13]. Decorrelation in the closed signal loop will either lead to unacceptable signal distortion (in the case of frequency shifting [8,10,11], half-wave rectification [20], and noise injection [7,9,20]), or will not be capable of providing sufficient decorrelation for tonal near-end signals (in the case of delay [10,12], all-pass filtering [22], and psychoacoustically masked noise injection [15]). When performing decorrelation in the adaptive filtering circuit, cascading the adaptive filter with a delay [6,9,17] will also be insufficient for tonal signals, while indirect closed-loop identification [19] requires the injection of a reference signal, which is again undesirable in terms of signal quality. AFC techniques that include a prefiltering of the adaptive filter's input and desired signal with an inverse model of the near-end signal [13,14,16,18,21,23] have been designed particularly for near-end speech signals, where the near-end signal model is a low-order all-pole speech signal model. Finally, in a closed-loop scenario a tonal near-end signal generates a tonal loudspeaker signal, so that the adaptive filter input signal is also tonal, which may dramatically decrease its convergence speed [24, Chapter 9].

The aim of this paper is to develop a modification to existing prediction-error-method (PEM)-based AFC approaches [18,21,23], such that these become capable of dealing with tonal audio signals. The PEM-based AFC algorithms are based on the PEM for system identification [25, Chapter 3; 26, Chapter 7]. Decorrelation is performed by prefiltering the adaptive filter's input and desired output signal with a time-varying inverse model of the near-end signal, which is estimated by linear prediction (LP) of the feedback-compensated signal. The PEM-AF algorithm in Spriet et al. [18] was derived for hearing aid applications, featuring a recursive LP of the feedback-compensated signal, and involving some common model approximations which are only relevant for short acoustic feedback paths. In Rombouts et al. [21], the PEM-AFROW algorithm was proposed for room acoustic applications, featuring a batch (frame-based) LP, and inheriting its name from the fact that no model approximations are introduced such that the prefiltering operation only involves row operations in the loudspeaker signal data matrix. In van Waterschoot et al. [27], the PEM-AF and PEM-AFROW algorithms were shown to be special cases of a more general recursive prediction error (RPE) identification algorithm. A common feature of the PEM-AF, PEM-AFROW, and RPE algorithms is the low-order all-pole structure that is used for modeling the near-end signal, which is indeed appropriate for speech signals. However, this conventional LP model is usually not well suited for tonal audio signals, which can be modeled more efficiently as a sum of sinusoids plus noise. It is well known that a signal consisting of sinusoids in noise admits a pole-zero rather than an all-pole representation [28,29]. As a consequence, the existing PEM-based AFC algorithms can be applied to audio signals only if the all-pole near-end signal model order is chosen very large. This would however lead to a dramatic increase of the computational requirements for the PEM-AF, PEM-AFROW, and RPE algorithms and to a violation of the PEM-AF stationarity assumptions in time-varying acoustic environments. In van Waterschoot and Moonen [30], we have investigated several alternative LP models for audio signals: selective all-pole models, pitch prediction all-pole models, frequency-warped all-pole models, and pole-zero models. Some of these alternative models appear to be capable of generating a "whiter", i.e., less correlated LP residual than the conventional low-order all-pole model, especially when cascaded with a conventional LP model. This observation is exploited in the current paper to derive a set of new AFC algorithms that can also handle tonal near-end signals. The proposed algorithms feature a cascade of two near-end signal models, a first one for predicting the tonal components and a second one for predicting the "noise-like" components in the near-end signal. The noise components model is chosen to be a conventional low-order all-pole model, while the tonal components model can be any of the alternative LP models described in van Waterschoot and Moonen [30]. An additional advantage of the proposed algorithms is that, by prefiltering the adaptive filter's input signal with the cascaded inverse near-end signal models, the tonal components in the input signal are also (partially) removed, and hence the adaptive filter's convergence is further improved.

This paper is organized as follows. In Section 2, the acoustic feedback problem is described in a discrete-time signal processing context, and the AFC concept is explained. In Section 3, we introduce a prediction error minimization criterion that features a cascade of two near-end signal models, and outline the proposed AFC algorithm. Also, an overview is given of the possible model structures for the near-end tonal components. In Section 4, we rederive the identifiability conditions given in Spriet et al. [18] for the PEM-AF algorithm, for the case of cascaded near-end signal models, resulting in the requirement of inserting processing delays at appropriate positions either in the closed signal loop or in the adaptive filtering circuit. Then in Section 5, algorithmic details of the PEM-based AFC approach with cascaded near-end signal models are given for different near-end tonal components model structures. Section 6 deals with computational complexity and contains an overview of the model approximations that can be applied for

decreasing the complexity. In Section 7, we illustrate the performance of the proposed algorithms by means of simulation results in both PA and HA scenarios. Finally, Section 8 concludes the paper.

2. Adaptive feedback cancellation

2.1. Problem description

The acoustic feedback problem is depicted in Fig. 1(a) for a setup with one microphone and one loudspeaker. In this setup, we refer to the source signal $v(t)$ as the near-end signal, and to the loudspeaker signal $u(t)$ as the far-end signal (adopting terminology from acoustic echo cancellation). The acoustic feedback path $F\{\cdot\}$ is defined as a function that maps the far-end signal $u(t)$ to the feedback signal $x(t)$, and is typically assumed to be linear, (slowly) time-varying, and of finite order n_F, i.e.,

$$F(q,t) = f_0(t) + f_1(t)q^{-1} + \cdots + f_{n_F}(t)q^{-n_F} \tag{1}$$

where $t \in \mathbb{Z}$ denotes the discrete time variable after sampling at sampling frequency $f_s = 1/T_s$, and q denotes the time shift operator, i.e., $q^{-k}u(t) = u(t-k)$. The electro-acoustic forward path $G\{\cdot\}$ maps the microphone signal $y(t) = v(t) + x(t)$ to the far-end signal $u(t)$ and is defined as the cascade of the characteristics of the microphone, the A/D converter, the amplifier, the D/A converter, the loudspeaker, and any signal processing device that is inserted in the signal loop, such as an equalizer and a compressor. The forward path mapping is typically non-linear for large signal amplitudes, due to amplifier or loudspeaker saturation, or because of compression. In the closed-loop system analysis, however, it is usually assumed that the forward path mapping is linear and time-varying, i.e.,

$$G(q,t) = g_1(t)q^{-1} + \cdots + g_{n_G}(t)q^{-n_G} \tag{2}$$

and possibly of infinite order ($n_G \to \infty$). Note that the forward path is assumed to contain (at least) one unit delay, i.e., $g_0(t) \equiv 0$, to avoid an algebraic loop.

The far-end signal and the near-end signal are related by the so-called closed-loop transfer function as follows:

$$u(t) = \frac{G(q,t)}{1 - G(q,t)F(q,t)}v(t) \tag{3}$$

According to Nyquist's stability criterion [31], the closed-loop system becomes unstable if there exists a radial frequency ω for which

$$\begin{cases} |G(e^{j\omega},t)F(e^{j\omega},t)| \geq 1 & (4) \\ \angle G(e^{j\omega},t)F(e^{j\omega},t) = n2\pi, \quad n \in \mathbb{Z} & (5) \end{cases}$$

where the short-time frequency responses $G(e^{j\omega},t)$ and $F(e^{j\omega},t)$ of the forward and feedback path, respectively, are obtained using the short-time Fourier transform (STFT). Except for the phase-modulated feedback control methods (see van Waterschoot and Moonen [1] for an overview), most of the existing methods for acoustic feedback control attempt to avoid the magnitude condition in (4) from being met for any $\omega \in [0,\pi]$, disregarding the phase condition (5). The maximum stable gain is defined as the electro-acoustic forward path gain value at which the point of instability of the closed-loop system is attained, and is usually determined in an experimental way, see, e.g., Maxwell and Zurek [9] and Spriet et al. [32]. If the amplifier's broadband gain factor $K(t)$ is factored out from the forward path transfer function, i.e.,

$$G(q,t) = K(t)J(q,t) \tag{6}$$

and if $\mathscr{P}$ denotes the set of frequencies at which the phase condition (5) is met, i.e.,

$$\mathscr{P} = \{\omega | \angle G(e^{j\omega},t)F(e^{j\omega},t) = n2\pi\} \tag{7}$$

then the maximum stable gain (MSG) can be formally defined as follows:

$$\mathrm{MSG}(t)\ [\mathrm{dB}] = -20\log_{10}\left[\max_{\omega\in\mathscr{P}} |J(e^{j\omega},t)F(e^{j\omega},t)|\right] \tag{8}$$

2.2. Adaptive feedback cancellation

The AFC concept consists in placing an FIR adaptive filter $\hat{F}(q,t)$ in parallel with the acoustic feedback path, having the far-end signal as its input and the microphone signal as its desired signal, see Fig. 1(b). The feedback signal $x(t)$ is then predicted by the adaptive filter output signal $\hat{y}[t|\hat{\mathbf{f}}(t)] = \hat{F}(q,t)u(t)$, which is subtracted from the microphone signal to deliver the feedback-compensated signal $d[t,\hat{\mathbf{f}}(t)] = y(t) - \hat{y}[t|\hat{\mathbf{f}}(t)]$, with

$$\hat{\mathbf{f}}(t) \triangleq [\hat{f}_0(t)\ ,\ldots,\ \hat{f}_{n_F}(t)]^T \tag{9}$$

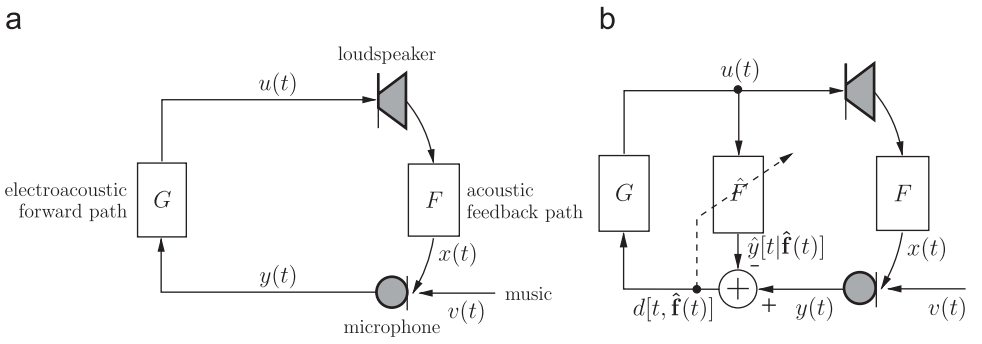

Fig. 1. (a) Acoustic feedback problem in 1-microphone/1-loudspeaker setup and (b) adaptive feedback cancellation concept.

Throughout this paper, we will assume that the acoustic feedback path model order n_F is known and that the adaptive filter order is equal to n_F. Note that the PEM-based AFC approach introduced in Section 3 has been shown to reduce the undermodeling bias and variance that tend to occur in the insufficient order case ($n_{\hat{F}} < n_F$) [33]. The closed-loop transfer function of the system with AFC is given by

$$u(t) = \frac{G(q,t)}{1 - G(q,t)[F(q,t) - \hat{F}(q,t)]} v(t) \tag{10}$$

such that the MSG can now be written as follows:

$$\mathrm{MSG}(t) = -20 \log_{10} \left[\max_{\omega} |J(e^{j\omega}, t)[F(e^{j\omega}, t) - \hat{F}(e^{j\omega}, t)]| \right] \tag{11}$$

and obviously increases when the mismatch between $\hat{F}(q,t)$ and $F(q,t)$ decreases. It is also expected that when $\hat{F}(q,t)$ approaches $F(q,t)$, the feedback-compensated signal $d[t, \hat{\mathbf{f}}(t)]$ will approach the near-end signal $v(t)$, which should lead to better sound quality [1].

3. PEM-based AFC

3.1. Data model

The estimation of the adaptive filter coefficients in $\hat{\mathbf{f}}(t)$ should be approached from a closed-loop system identification point of view. It is well known that if the near-end signal $v(t)$ is a correlated sequence, such as speech or music, then standard Wiener or least-squares (LS) estimation provides a biased solution [1,12,13,34]. An unbiased feedback path estimate can be obtained with the so-called direct method [34] when a model of the near-end signal is taken into account in the identification (corresponding to the "noise model" in system identification theory). The data model can then be written as

$$y(t) = F(q,t)u(t) + \overbrace{H(q,t)e(t)}^{v(t)} \tag{12}$$

with $e(t)$ an uncorrelated sequence such as Gaussian white noise or a Dirac impulse. However, because of the nonstationarity of speech and music signals, the near-end signal model $H(q,t)$ is time-varying and so should be estimated concurrently with the acoustic feedback path $F(q,t)$. This is possible by applying a prediction error system identification method [25, Chapter 3; 26, Chapter 7], as shown in [18,21,23,27]. Here, the near-end signal model is assumed to be an all-pole model, which is a relevant assumption for speech applications.

If the near-end signal is a tonal audio signal, then an all-pole model is usually not appropriate, but instead a cascade of two linear models may be used for the near-end signal [30]. The data model can then be rewritten as

$$y(t) = F(q,t)u(t) + H_1(q,t)H_2(q,t)e(t) \tag{13}$$

In the near-end signal model cascade, $H_1(q,t)$ is a model for the tonal components, while $H_2(q,t)$ is a model for the "noise-like" components. The noise components model is again chosen to be an all-pole model, i.e.,

$$H_2(q,t) = \frac{1}{C(q,t)} = \frac{1}{1 + c_1(t)q^{-1} + \cdots + c_{n_C}(t)q^{-n_C}} \tag{14}$$

which corresponds to the near-end speech model used in the estimation algorithms in [18,21,23,27]. The tonal components model can be any of the LP models described in van Waterschoot and Moonen [30]: an all-pole (LP) model, a selective all-pole (SLP) model, a pitch prediction (PLP) model, a frequency-warped all-pole (WLP) model, or a pole-zero (PZLP) model. Table 1 lists these five models, together with the corresponding prediction error filter (PEF) transfer functions and parameter vectors. Note that the parameter vectors $\boldsymbol{\alpha}(t)$, which contain the tonal components model parameters that have to be estimated in the PEM-based AFC algorithm, are not equivalent to the PEF impulse response vectors, which will be denoted as $\mathbf{a}(t)$. Also, the PEF order n_A is not necessarily equal to the number of elements in the parameter vector $\boldsymbol{\alpha}(t)$, which will be denoted by n_α. In the PZLP model, the numerator and denominator order are equal, and the poles and zeros are constrained to lie on the same radial lines in the z-plane, more specifically at angles $\theta_i(t)$, $i = 1, \ldots, n_A/2$. The fractional pitch lag $K - l/D$ (with $K \in \mathbb{Z}$ and $l = 0, \ldots, D-1$) in the fractional 3-tap PLP model can be implemented by using a fractional interpolation filter $I(q, l/D)$. The WLP and SLP models both have an all-pole structure in which the unit delay element has been transformed: in the SLP model the transformation consists in a

Table 1
Overview of near-end tonal components models.

Model	PEF transfer function	Parameter vector
LP	$A(q,t) = 1 + \sum_{i=1}^{n_A} a_i(t) q^{-i}$	$\boldsymbol{\alpha}(t) = [a_1(t), \ldots, a_{n_A}(t)]^T$
SLP	$A(q,t) = 1 + \sum_{i=1}^{n_A} \alpha_i(t) q^{-iL}$	$\boldsymbol{\alpha}(t) = [\alpha_1(t), \ldots, \alpha_{n_A}(t)]^T$
PLP	$A(q,t) = 1 - \sum_{i=-1}^{1} \alpha_i(t) q^{-K-(l/D)-i} = 1 - \sum_{i=-1}^{1} \alpha_i(t) I(q, l/D) q^{-K-i}$	$\boldsymbol{\alpha}(t) = [K, l, \alpha_{-1}(t), \alpha_0(t), \alpha_1(t)]^T$
WLP	$A(q,t) = D_0^{-1}(q,\lambda) \left[1 + \sum_{i=1}^{n_A} \alpha_i(t) D^i(q,\lambda) \right]$	$\boldsymbol{\alpha}(t) = [\alpha_1(t), \ldots, \alpha_{n_A}(t)]^T$
PZLP	$\frac{A(q,t)}{B(q,t)} = \prod_{i=1}^{n_A/2} \frac{1 - 2v_i \cos\theta_i q^{-1} + v_i^2 q^{-2}}{1 - 2\rho_i \cos\theta_i q^{-1} + \rho_i^2 q^{-2}}$	$\boldsymbol{\alpha}(t) = [\theta_1(t), \ldots, \theta_{n_A/2}(t)]^T$

downsampling operation (anti-aliasing filtering followed by decimation) with a factor Γ, while in the WLP the unit delay q^{-1} is replaced by a bilinear all-pass filter

$$D(q,\lambda)=\frac{q^{-1}-\lambda}{1-\lambda q^{-1}} \tag{15}$$

with warping parameter $\lambda\in(-1,1)$. The WLP model moreover features an initial whitening filter

$$D_0^{-1}(q,\lambda)=\frac{1-\lambda q^{-1}}{\sqrt{1-\lambda^2}} \tag{16}$$

to increase the residual's spectral flatness [35].

These five LP models were evaluated in van Waterschoot and Moonen [30] in terms of their frequency estimation accuracy, residual spectral flatness, and perceptual frequency resolution. In PEM-based AFC, the aim of including a near-end signal model is to whiten the near-end signal component in the microphone signal, hence an LP model providing a high residual spectral flatness is preferred. In the case of monophonic audio signals, the highest residual spectral flatness is obtained with the PLP and PZLP models, while for polyphonic audio signals the WLP model provides the highest spectral flattening [30]. For the sake of conciseness, we will focus on these three LP models in the rest of this paper. The identifiability conditions, algorithm details, and simulation results when using the other (LP and SLP) near-end tonal components models can be found in van Waterschoot [36, Chapter 12].

3.2. Prediction error identification algorithm

Using the data model in (13), the prediction error identification approach can be outlined as follows. The best one-step ahead predictor for $y(t)$ can be calculated, following [25, Chapter 3], as

$$\begin{aligned}\hat{y}[t|\boldsymbol{\xi}(t)]&=[1-H_2^{-1}(q,t)H_1^{-1}(q,t)]y(t)\\&\quad+H_2^{-1}(q,t)H_1^{-1}(q,t)F(q,t)u(t)\end{aligned} \tag{17}$$

with the parameter vector $\boldsymbol{\xi}(t)$ defined as

$$\boldsymbol{\xi}(t)\triangleq[\mathbf{f}^T(t)\ \ \boldsymbol{\gamma}^T(t)\ \ \boldsymbol{\alpha}^T(t)]^T \tag{18}$$

and

$$\mathbf{f}(t)\triangleq[f_0(t)\ \ ,\ldots,\ \ f_{n_F}(t)]^T \tag{19}$$

$$\boldsymbol{\gamma}(t)\triangleq[c_1(t)\ \ ,\ldots,\ \ c_{n_C}(t)]^T \tag{20}$$

and with $\boldsymbol{\alpha}(t)$ defined in Table 1. The prediction error defined as

$$\varepsilon[t,\boldsymbol{\xi}(t)]\triangleq y(t)-\hat{y}[t|\boldsymbol{\xi}(t)] \tag{21}$$

can hence be calculated as

$$\varepsilon[t,\boldsymbol{\xi}(t)]=H_2^{-1}(q,t)H_1^{-1}(q,t)[y(t)-F(q,t)u(t)] \tag{22}$$

The parameter vector $\boldsymbol{\xi}(t)$ can be estimated by minimizing the sum of squared prediction errors,

$$\min_{\boldsymbol{\xi}(t)}\frac{1}{2N}\sum_{k=1}^{t}\zeta^{-1}(k,t)\varepsilon^2[k,\boldsymbol{\xi}(t)] \tag{23}$$

with $\zeta^{-1}(k,t)$ a weighting factor for discounting old data and compensating for power variations in the near-end excitation signal $e(t)$, and N denoting the effective window length after data weighting.

In AFC, it is considered advantageous to decouple the identification of $F(q,t)$, $H_1(q,t)$, and $H_2(q,t)$. This allows for using data windows of different length [18] and applying different estimation methods [21] for the identification of the acoustic feedback path and the near-end signal models. It has been shown that this approach results in an estimate $\hat{\boldsymbol{\xi}}(t)$ that corresponds to a local minimum of the criterion in (23), but not necessarily to the global minimum [21,27]. It was found in van Waterschoot et al. [27] that a smaller near-end signal model order increases the probability of finding the global solution, which is yet another motivation for using a cascade of two low-order near-end signal models rather than a single high-order all-pole model. The identification of $F(q,t)$, $H_1(q,t)$, and $H_2(q,t)$ can be decoupled by performing the minimization of (23) in three stages:

(1) Estimation of $H_1(q,t)$: using (14), we can rewrite (22) as

$$H_1(q,t)\varepsilon[t,\boldsymbol{\xi}(t)]=C(q,t)[y(t)-F(q,t)u(t)] \tag{24}$$

$$\triangleq w[t,\boldsymbol{\gamma}(t),\mathbf{f}(t)] \tag{25}$$

The near-end tonal components model $H_1(q,t)$ can then be estimated using an appropriate LP method for predicting $w[t,\boldsymbol{\gamma}(t),\mathbf{f}(t)]$, and replacing the parameter vectors $\boldsymbol{\gamma}(t)$ and $\mathbf{f}(t)$ by recently obtained estimates, see Section 5 for a detailed treatment. Note that the prefiltering operation with $C(q,t)$ in (24) is expected to whiten the near-end noise components in the feedback-compensated signal $y(t)-F(q,t)u(t)$, which facilitates the estimation of the near-end tonal components model $H_1(q,t)$.

(2) Estimation of $H_2(q,t)$: rewriting (22) with (14) as

$$C^{-1}(q,t)\varepsilon[t,\boldsymbol{\xi}(t)]=H_1^{-1}(q,t)[y(t)-F(q,t)u(t)] \tag{26}$$

$$\triangleq r[t,\boldsymbol{\alpha}(t),\mathbf{f}(t)] \tag{27}$$

reveals that the near-end noise components model $H_2(q,t)=C^{-1}(q,t)$ can be estimated by LP of $r[t,\boldsymbol{\alpha}(t),\mathbf{f}(t)]$, with $\boldsymbol{\alpha}(t)$ and $\mathbf{f}(t)$ replaced by recent estimates, see Section 5. Since the near-end tonal components in the feedback-compensated signal $y(t)-F(q,t)u(t)$ are cancelled by the prefiltering with $H_1^{-1}(q,t)$, these do not disturb the near-end noise components model estimation.

(3) Estimation of $F(q,t)$: if we define the following prefiltered far-end and microphone signals:

$$\tilde{u}[t,\boldsymbol{\alpha}(t),\boldsymbol{\gamma}(t)]\triangleq C(q,t)H_1^{-1}(q,t)u(t) \tag{28}$$

$$\tilde{y}[t,\boldsymbol{\alpha}(t),\boldsymbol{\gamma}(t)]\triangleq C(q,t)H_1^{-1}(q,t)y(t) \tag{29}$$

then the minimization of the sum of squared prediction errors in (23) w.r.t. $\boldsymbol{\xi}(t)$ can be rewritten as a standard LS minimization w.r.t. $\mathbf{f}(t)$

$$\min_{\mathbf{f}(t)}\frac{1}{2N}\sum_{k=1}^{t}\zeta^{-1}(k,t)\{\tilde{y}[t,\boldsymbol{\alpha}(t),\boldsymbol{\gamma}(t)]-F(q,t)\tilde{u}[t,\boldsymbol{\alpha}(t),\boldsymbol{\gamma}(t)]\}^2 \tag{30}$$

in which the parameter vectors $\boldsymbol{\alpha}(t)$ and $\boldsymbol{\gamma}(t)$ may be replaced by recently obtained estimates, see Section 5. In the LS problem defined in (30), the near-end signal component in the microphone signal has been whitened by prefiltering with $C(q,t)H_1^{-1}(q,t)$ such that an unbiased estimate of the acoustic feedback path can be obtained. A beneficial side effect of this approach is that the tonal components in the far-end signal, whose frequencies can be assumed to be equal to the near-end tonal component frequencies since the electro-acoustic forward path is modeled as a linear system $G(q,t)$, are (partially) cancelled by prefiltering with $H_1^{-1}(q,t)$, which improves the conditioning of the LS problem in (30).

4. Identifiability conditions

Before presenting the details of the PEM-based AFC algorithm with cascaded near-end signal models, it is necessary to derive the conditions under which the models $F(q,t)$, $H_1(q,t)$, and $H_2(q,t)$ are jointly identifiable from the LS criterion in (22) and (23). This derivation differs depending on which tonal components model is used.

4.1. PLP near-end tonal components model

When the PLP near-end tonal components model is used, the inverse model $H_1^{-1}(q,t)$ has a finite-order all-zero parametrization, such that the inverse cascaded near-end signal models $H_1^{-1}(q,t)=A(q,t)$ and $H_2^{-1}(q,t)=C(q,t)$ form a single all-zero model $D(q,t)\triangleq C(q,t)A(q,t)$ of order $n_D=n_A+n_C$, and the identifiability conditions derived in Spriet et al. [18] can be applied. In this case, $F(q,t)$ and $D(q,t)$ are jointly identifiable if all of the following conditions are satisfied [18]:

(1) the near-end signal admits an autoregressive (AR) representation of order n_D or less,
(2) processing delays of d_1 and d_2 samples are inserted in the electro-acoustic forward path $G(q,t)$ and in the adaptive filtering circuit, respectively, with $d_1+d_2\geq n_D+1$,
(3) the acoustic feedback path has an initial delay of at least d_2T_s s due to the time needed for the sound to travel in a direct path from the loudspeaker to the microphone.

Note that these conditions do not guarantee the unique identification of $C(q,t)$ and $A(q,t)$, since all the zeros of these polynomials are identified together in the cascade model $D(q,t)$. However, this should not be a problem since the identification of $C(q,t)$ and $A(q,t)$ is not of primary interest, but merely serves as an auxiliary procedure for consistently identifying $F(q,t)$.

4.2. WLP near-end tonal components model

The WLP PEF can either be implemented as an IIR filter, or be as a warped FIR filter [35]. In the latter case, the derivation of the identifiability conditions is similar to the derivation in Spriet et al. [18], resulting in the requirements that

(1) the near-end signal admits a mixed conventional/frequency-warped AR representation of orders n_C and n_A or less, respectively,
(2) processing delays d_1 and d_2 are inserted with $d_1+d_2\geq n_A+n_C+1$,
(3) the acoustic feedback path has an initial delay of at least d_2T_s s.

4.3. PZLP near-end tonal components model

The PZLP near-end tonal components model $H_1(q,t)=B(q,t)/A(q,t)$ is jointly identifiable with the noise components model $H_2(q,t)=1/C(q,t)$ and the acoustic feedback path $F(q,t)$ if all of the following conditions are satisfied:

(1) the near-end signal admits an autoregressive moving average (ARMA) representation with the AR and MA orders less than or equal to n_A+n_C and n_A, respectively,
(2) processing delays d_1 and d_2 are inserted with $d_1+d_2\geq n_A+n_C+1$,
(3) the acoustic feedback path has an initial delay of at least d_2T_s s.

These conditions can be derived as follows. In the PZLP case, the prediction error can be written as

$$\varepsilon[t,\boldsymbol{\xi}(t)]=C(q,t)\frac{A(q,t)}{B(q,t)}[y(t)-F(q,t)u(t)] \tag{31}$$

The LS problem (23) related to (31) can be rewritten as a three-channel identification problem, see Fig. 2, by rewriting (31) as

$$\varepsilon[t,\boldsymbol{\xi}(t)]=\underbrace{C(q,t)A(q,t)}_{\triangleq D(q,t)}y(t)-\underbrace{C(q,t)A(q,t)F(q,t)}_{\triangleq -L(q,t)}u(t)+\underbrace{[1-B(q,t)]}_{\triangleq -q^{-1}\bar{B}(q,t)}\varepsilon[t,\boldsymbol{\xi}(t)] \tag{32}$$

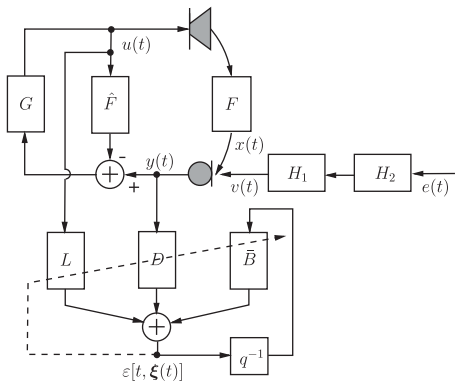

Fig. 2. Three-channel identification scheme for determining the identifiability conditions with a PZLP near-end tonal components model.

Using (10) and $y(t)=F(q,t)u(t)+v(t)$, we can rewrite (32) as

$$\varepsilon[t,\xi(t)]=\frac{D(q,t)+G(q,t)[L(q,t)+\hat{F}(q,t)D(q,t)]}{1-G(q,t)[F(q,t)-\hat{F}(q,t)]}v(t) - q^{-1}\bar{B}(q,t)\varepsilon[t,\xi(t)] \quad (33)$$

Let us again assume that the forward path and the adaptive filtering circuit contain processing delays of d_1 and d_2 samples, respectively, and that the acoustic feedback path has an initial delay of at least d_2T_s s. Under these assumptions, the following equalities hold:

$$G(q,t)=q^{-d_1}\bar{G}(q,t) \text{ with } \bar{G}(q,t) \triangleq g_{d_1}+g_{d_1+1}q^{-1}+\cdots+g_{n_G}q^{-n_G+d_1} \quad (34)$$

$$F(q,t)=q^{-d_2}\bar{F}(q,t) \text{ with } \bar{F}(q,t) \triangleq f_{d_2}+f_{d_2+1}q^{-1}+\cdots+f_{n_F}q^{-n_F+d_2} \quad (35)$$

$$\hat{F}(q,t)=q^{-d_2}\hat{\bar{F}}(q,t) \text{ with } \hat{\bar{F}}(q,t) \triangleq \hat{f}_{d_2}+\hat{f}_{d_2+1}q^{-1}+\cdots+\hat{f}_{n_F}q^{-n_F+d_2} \quad (36)$$

$$L(q,t)=q^{-d_2}\bar{L}(q,t) \text{ with } \bar{L}(q,t) \triangleq l_{d_2}+l_{d_2+1}q^{-1}+\cdots+l_{n_L}q^{-n_L+d_2} \quad (37)$$

with $n_L=n_A+n_C+n_F$, and hence (33) can be rewritten as follows:

$$\begin{aligned}\varepsilon[t,\xi(t)] &= \frac{D(q,t)+q^{-(d_1+d_2)}\bar{G}(q,t)[\bar{L}(q,t)+\hat{\bar{F}}(q,t)D(q,t)]}{1-q^{-(d_1+d_2)}\bar{G}(q,t)[\bar{F}(q,t)-\hat{\bar{F}}(q,t)]}v(t) \\ &\quad - q^{-1}\bar{B}(q,t)\varepsilon[t,\xi(t)] \\ &= \{D(q,t)+q^{-(d_1+d_2)}\bar{G}(q,t)[\bar{L}(q,t)+\hat{\bar{F}}(q,t)D(q,t)]\}v(t) \\ &\quad - \{q^{-1}\bar{B}(q,t)-q^{-(d_1+d_2)}\bar{G}(q,t)[\bar{F}(q,t) \\ &\quad - \hat{\bar{F}}(q,t)]B(q,t)\}\varepsilon[t,\xi(t)] \end{aligned} \quad (38)$$

If the near-end signal admits an ARMA representation $D_0(q,t)/B_0(q,t)$ with the AR and MA orders less than or equal to n_D and n_B, respectively, then the solution to the LS problem (23) with (38) is equal to the desired solution if

$$d_1+d_2 \geq \max\{n_D,n_B\}+1 \quad (39)$$

$$\geq n_A+n_C+1 \quad (40)$$

where the latter inequality follows from the fact that we have constrained the PZLP model denominator and numerator order to be equal, see Section 3.1. Indeed, it can be verified that in this case the solution to (23) and (38) corresponds to

$$\begin{cases} D(q,t)=D_0(q,t) & (41) \\ \bar{G}(q,t)[\bar{L}(q,t)+\hat{\bar{F}}(q,t)D(q,t)]\equiv 0 & \\ \quad \Leftrightarrow \bar{L}(q,t)\equiv -\hat{\bar{F}}(q,t)D(q,t) & (42) \\ B(q,t)=B_0(q,t) & (43) \\ \bar{G}(q,t)[\bar{F}(q,t)-\hat{\bar{F}}(q,t)]B(q,t)\equiv 0 & \\ \quad \Leftrightarrow \bar{F}(q,t)\equiv \hat{\bar{F}}(q,t) & (44) \end{cases}$$

Note that, as was the case for the PLP model, an unavoidable ambiguity exists between the zeros of the PZLP near-end tonal components model PEF $A(q,t)/B(q,t)$ and the noise components model PEF $C(q,t)$, which are combined in the cascade model $D(q,t)$.

Finally, also note that an example of a signal admitting an ARMA(n_D,n_B) representation is a signal consisting of a sum of sinusoids in AR noise, i.e.,

$$v(t)=\sum_{n=1}^{N}\beta_n\cos(\omega_n t+\phi_n)+\frac{1}{C(q,t)}e(t) \quad (45)$$

As shown in Chan et al. [29], the linear prediction property of a sum of N sinusoidal signals leads to an ARMA($2N,2N$) representation in white noise, which can be extended to an ARMA($2N+n_C,2N$) representation in AR(n_C) noise.

5. Algorithm details

In the existing PEM-AF [18] and RPE [27] algorithms, the near-end signal model $H(q,t)$ is identified recursively, while the PEM-AFROW [21] algorithm features a batch near-end signal model identification. It has been found that the latter approach is more robust, since a recursive near-end signal model identification may result in numerical problems due to a scaling ambiguity that is inherent in the PEM-based approach [37]. Moreover, efficient batch estimation methods for identifying the near-end tonal components models in Table 1 are readily available in the literature, see van Waterschoot and Moonen [30] for an overview. For these reasons, we will only consider batch estimation of the near-end tonal and noise components models $H_1(q,t)$ and $H_2(q,t)$. Moreover, we will assume that $H_1(q,t)$ and $H_2(q,t)$ are piecewise stationary on similar time scales, such that both models can be identified on data windows of the same size. More specifically, we will use data windows that have a length of M samples and a hop size of P samples. Moreover, the data window is positioned in time such that it contains $P-1$ future samples and $M-P$ past samples. The choice of M and P are crucial for the AFC algorithm performance: M should be chosen large enough to obtain low-variance estimates of the parameters of $H_1(q,t)$ and $H_2(q,t)$, but not too large such that the models themselves can be assumed stationary in the entire data window. For LP of audio signals, data windows of 40–60 ms appear to be well suited [30]. The hop size P could theoretically be chosen nearly as large as the data window length M (a minimal difference of $M-P=n_C$ will appear to be necessary, as shown below); however, it should be taken into account that a processing delay of $P-1$ samples has to be inserted in the forward path $G(q,t)$ to preserve causality in the AFC algorithm. We will typically choose $P=M/2$, such that successive LP data windows have a 50% overlap. This choice implies that the forward path contains a delay corresponding to 20–30 ms. From a perceptual point of view, a forward path delay of 20–30 ms should be acceptable in PA applications since the typical distance-values between the loudspeakers and the audience introduce similar delay values. In HA applications, inserting a forward path delay introduces a time offset between the so-called "bone-conducted" sound signal and the "aid-conducted" sound signal. Delays of 20–30 ms (or higher for severely hearing-impaired subjects) were found

to be acceptable in terms of speech quality [38]; however, no results for audio signals have been reported.

The PEM-based AFC algorithms with cascaded near-end signal models presented here are recursive algorithms in which each recursion consists of a sequence of nine operations:

for t
  if $j = t \bmod P = 0$
    (1) calculation of a priori feedback-compensated signal $d[t,\hat{\mathbf{f}}(t-1)]$ for the entire LP data window
    (2) calculation of prefiltered data vector $\mathbf{w}[t,\hat{\gamma}(t-P),\hat{\mathbf{f}}(t-1)]$
    (3) batch estimation of $\hat{\boldsymbol{\alpha}}(t)$ using $\mathbf{w}[t,\hat{\gamma}(t-P),\hat{\mathbf{f}}(t-1)]$
    (4) calculation of prefiltered data vector $\mathbf{r}[t,\hat{\boldsymbol{\alpha}}(t),\hat{\mathbf{f}}(t-1)]$
    (5) batch estimation of $\hat{\gamma}(t)$ using $\mathbf{r}[t,\hat{\boldsymbol{\alpha}}(t),\hat{\mathbf{f}}(t-1)]$
  end if
    (6) calculation of prediction error $\varepsilon[t,\hat{\boldsymbol{\alpha}}(t-j),\hat{\gamma}(t-j),\hat{\mathbf{f}}(t-1)]$ and prefiltered data vector $\tilde{\mathbf{u}}[t,\hat{\boldsymbol{\alpha}}(t-j),\hat{\gamma}(t-j)]$
    (7) recursive estimation of prediction error power $\sigma^2(t)$
    (8) recursive estimation of $\hat{\mathbf{f}}(t)$ using $\varepsilon[t,\hat{\boldsymbol{\alpha}}(t-j),\hat{\gamma}(t-j),\hat{\mathbf{f}}(t-1)]$ and $\tilde{\mathbf{u}}[t,\hat{\boldsymbol{\alpha}}(t-j),\hat{\gamma}(t-j)]$
    (9) calculation of a posteriori feedback-compensated signal $d[t,\hat{\mathbf{f}}(t)]$
end for

The prefiltering and LP estimation details are different depending on the near-end tonal components model used, and will be described for the different cases.

5.1. PLP near-end tonal components model

If the near-end tonal components model has an all-zero PEF, i.e., for the PLP model, the above nine operations can be described as shown in Table 2. The impulse response coefficients of the PEFs $\hat{A}(q,t)$ and $\hat{C}(q,t)$ are collected in the vectors $\hat{\mathbf{a}}(t)$ and $\hat{\mathbf{c}}(t)$, respectively, which are different from—but related to—parameter vectors $\hat{\boldsymbol{\alpha}}(t)$ and $\hat{\gamma}(t)$ (see (20) and Table 1). Note that for the calculation of $\varepsilon[t,\hat{\boldsymbol{\alpha}}(t),\hat{\gamma}(t),\hat{\mathbf{f}}(t-1)]$ from $r[k,\hat{\boldsymbol{\alpha}}(t),\hat{\mathbf{f}}(t-1)]$, $k\in[t-n_C,t]$ in step 6a), it is required that $P\leq M-n_C$.

The recursive estimation of the acoustic feedback path parameter vector $\hat{\mathbf{f}}(t)$ in step 8 of the PEM-based AFC algorithm is carried out using a normalized least mean squares (NLMS)-like update equation, using the prefiltered far-end signal vector $\tilde{\mathbf{u}}[t,\hat{\boldsymbol{\alpha}}(t),\hat{\gamma}(t)]$ instead of the original far-end signal vector (as would be used in a standard NLMS-based AFC algorithm). Apart from the normalization factor $\tilde{\mathbf{u}}^T\tilde{\mathbf{u}}$, the estimated prediction error power $\sigma^2(t)$ and the regularization parameter δ also appear in the denominator of the update term. Three estimates of the prediction error power [$\sigma_A^2(t)$, $\sigma_{\hat{C}}^2(t)$, and $\sigma_{\hat{e}}^2(t)$] are available in the algorithm, and these are averaged to obtain the prediction error power estimate $\sigma^2(t)$ that is used in the update equation for $\hat{\mathbf{f}}(t)$.

Table 2
PEM-based AFC algorithm: PLP near-end tonal components model.

for t
  if $j = t \bmod P = 0$

(1) $d[k,\hat{\mathbf{f}}(t-1)] = y(k) - [u(k) \;\; \dots \;\; u(k-n_F)]\hat{\mathbf{f}}(t-1), \quad k\in[t+P-M-\max(n_A,n_C),t+P-1]$

(2) $$\mathbf{w}[t,\hat{\gamma}(t-P),\hat{\mathbf{f}}(t-1)] = \begin{bmatrix} d[t+P-M,\hat{\mathbf{f}}(t-1)] & \dots & d[t+P-M-n_C,\hat{\mathbf{f}}(t-1)] \\ \vdots & \ddots & \vdots \\ d[t+P-1,\hat{\mathbf{f}}(t-1)] & \dots & d[t+P-1-n_C,\hat{\mathbf{f}}(t-1)] \end{bmatrix}\hat{\mathbf{c}}(t-P)$$

(3) $\{\hat{\boldsymbol{\alpha}}(t),\sigma_A^2(t)\} = \mathrm{plp}\{\mathbf{w}[t,\hat{\gamma}(t-P),\hat{\mathbf{f}}(t-1)]\}$

(4) $$\mathbf{r}[t,\hat{\boldsymbol{\alpha}}(t),\hat{\mathbf{f}}(t-1)] = \begin{bmatrix} d[t+P-M,\hat{\mathbf{f}}(t-1)] & \dots & d[t+P-M-n_A,\hat{\mathbf{f}}(t-1)] \\ \vdots & \ddots & \vdots \\ d[t+P-1,\hat{\mathbf{f}}(t-1)] & \dots & d[t+P-1-n_A,\hat{\mathbf{f}}(t-1)] \end{bmatrix}\hat{\mathbf{a}}(t)$$

(5) $\{\hat{\gamma}(t),\sigma_{\hat{C}}^2(t)\} = \mathrm{lp}\{\mathbf{r}[t,\hat{\boldsymbol{\alpha}}(t),\hat{\mathbf{f}}(t-1)]\}$

(6a)
$$\begin{cases} \varepsilon[t,\hat{\boldsymbol{\alpha}}(t),\hat{\gamma}(t),\hat{\mathbf{f}}(t-1)] = \begin{bmatrix} r[t,\hat{\boldsymbol{\alpha}}(t),\hat{\mathbf{f}}(t-1)] & \dots & r[t-n_C,\hat{\boldsymbol{\alpha}}(t),\hat{\mathbf{f}}(t-1)] \end{bmatrix}\hat{\mathbf{c}}(t) \\ \breve{u}[k,\hat{\boldsymbol{\alpha}}(t)] = \begin{bmatrix} u(k) & \dots & u(k-n_A) \end{bmatrix}\hat{\mathbf{a}}(t), \quad k\in[t-n_F-n_C,t+P-1] \\ \breve{y}[k,\hat{\boldsymbol{\alpha}}(t)] = \begin{bmatrix} y(k) & \dots & y(k-n_A) \end{bmatrix}\hat{\mathbf{a}}(t), \quad k\in[t-n_C+1,t+P-1] \\ \tilde{\mathbf{u}}[t,\hat{\boldsymbol{\alpha}}(t),\hat{\gamma}(t)] = \begin{bmatrix} \tilde{u}[t,\hat{\boldsymbol{\alpha}}(t),\hat{\gamma}(t)] \\ \vdots \\ \tilde{u}[t-n_F,\hat{\boldsymbol{\alpha}}(t),\hat{\gamma}(t)] \end{bmatrix} = \begin{bmatrix} \breve{u}[t,\hat{\boldsymbol{\alpha}}(t)] & \dots & \breve{u}[t-n_C,\hat{\boldsymbol{\alpha}}(t)] \\ \vdots & \ddots & \vdots \\ \breve{u}[t-n_F,\hat{\boldsymbol{\alpha}}(t)] & \dots & \breve{u}[t-n_F-n_C,\hat{\boldsymbol{\alpha}}(t)] \end{bmatrix}\hat{\mathbf{c}}(t) \end{cases}$$

  else

(6b)
$$\begin{cases} \tilde{u}[t,\hat{\boldsymbol{\alpha}}(t-j),\hat{\gamma}(t-j)] = \begin{bmatrix} \breve{u}[t,\hat{\boldsymbol{\alpha}}(t-j)] & \dots & \breve{u}[t-n_C,\hat{\boldsymbol{\alpha}}(t-j)] \end{bmatrix}\hat{\mathbf{c}}(t-j) \\ \tilde{y}[t,\hat{\boldsymbol{\alpha}}(t-j),\hat{\gamma}(t-j)] = \begin{bmatrix} \breve{y}[t,\hat{\boldsymbol{\alpha}}(t-j)] & \dots & \breve{y}[t-n_C,\hat{\boldsymbol{\alpha}}(t-j)] \end{bmatrix}\hat{\mathbf{c}}(t-j) \\ \tilde{\mathbf{u}}[t,\hat{\boldsymbol{\alpha}}(t-j),\hat{\gamma}(t-j)] = \begin{bmatrix} \tilde{u}[t,\hat{\boldsymbol{\alpha}}(t-j),\hat{\gamma}(t-j)] & \dots & \tilde{u}[t-n_F,\hat{\boldsymbol{\alpha}}(t-j),\hat{\gamma}(t-j)] \end{bmatrix}^T \\ \varepsilon[t,\hat{\boldsymbol{\alpha}}(t-j),\hat{\gamma}(t-j),\hat{\mathbf{f}}(t-1)] = \tilde{y}[t,\hat{\boldsymbol{\alpha}}(t-j),\hat{\gamma}(t-j)] - \tilde{\mathbf{u}}^T[t,\hat{\boldsymbol{\alpha}}(t-j),\hat{\gamma}(t-j)]\hat{\mathbf{f}}(t-1) \end{cases}$$

  end if

(7)
$$\begin{cases} \sigma_{\hat{e}}^2(t) = \lambda_{\varepsilon}\sigma_{\hat{e}}^2(t-1) + (1-\lambda_{\varepsilon})\varepsilon^2[t,\hat{\boldsymbol{\alpha}}(t-j),\hat{\gamma}(t-j),\hat{\mathbf{f}}(t-1)] \\ \sigma^2(t) = [\sigma_A^2(t-j) + \sigma_{\hat{C}}^2(t-j) + \sigma_{\hat{e}}^2(t)]/3 \end{cases}$$

(8) $$\hat{\mathbf{f}}(t) = \hat{\mathbf{f}}(t-1) + \mu\frac{\tilde{\mathbf{u}}[t,\hat{\boldsymbol{\alpha}}(t-j),\hat{\gamma}(t-j)]\varepsilon[t,\hat{\boldsymbol{\alpha}}(t-j),\hat{\gamma}(t-j),\hat{\mathbf{f}}(t-1)]}{\tilde{\mathbf{u}}^T[t,\hat{\boldsymbol{\alpha}}(t-j),\hat{\gamma}(t-j)]\tilde{\mathbf{u}}[t,\hat{\boldsymbol{\alpha}}(t-j),\hat{\gamma}(t-j)] + \sigma^2(t) + \delta}$$

(9) $d[t,\hat{\mathbf{f}}(t)] = y(t) - \begin{bmatrix} u(t) & \dots & u(t-n_F) \end{bmatrix}\hat{\mathbf{f}}(t)$

end for

In Table 2, we have omitted the actual algorithms for estimating the LP and PLP model coefficients. The estimation of LP model coefficients is a well-known problem, which is readily solved by estimating a set of autocorrelation coefficients and subsequently solving a linear system of equations, see e.g., Makhoul [39]. Estimating the coefficients of the fractional 3-tap PLP model coefficients can be done by applying a two-step pitch prediction algorithm. First the pitch lag K and fractional phase l are estimated by performing an exhaustive search for the minimal fractional 1-tap PLP residual power in the two-dimensional grid defined by $K \in \{[K_{\min}, K_{\max}] \cap \mathbb{Z}\}$ and $l \in \{[0, D-1] \cap \mathbb{Z}\}$ [40,41]. The fractional 3-tap PLP model coefficients are then estimated by calculating the autocorrelation coefficients for lags around the previously estimated fractional pitch lag value $K + l/D$, and subsequently solving a linear system of equations. This system of equations can be forced to be Toeplitz or diagonal to speed up the estimation [42].

5.2. WLP near-end tonal components model

Since the WLP PEF $A(q,t)$ has an infinite impulse response, the algorithm in Table 2 cannot be used when the tonal components model has the WLP model structure. It was shown in van Waterschoot and Moonen [43] that an efficient recursive AFC algorithm can be obtained in this case by performing the prefiltering operations involving $A(q,t)$ directly in the warped domain. This is possible because an IIR WLP PEF can be implemented as a warped FIR filter [35], which has a finite number of filter states. The approach in van Waterschoot and Moonen [43] can be extended with a cascaded near-end noise components model, resulting in the algorithm shown in Table 3. The main difference with the algorithm in Table 2 is found in step 4, where the signals $\breve{u}[k, \hat{\boldsymbol{\alpha}}(t)]$ and $\breve{y}[k, \hat{\boldsymbol{\alpha}}(t)]$ are computed as an intermediate step before calculating the prefiltered data vectors $\mathbf{r}[t, \hat{\boldsymbol{\alpha}}(t), \hat{\mathbf{f}}(t-1)]$ and $\tilde{\mathbf{u}}[t, \hat{\boldsymbol{\alpha}}(t), \hat{\gamma}(t)]$. The far-end and microphone signals $u(k)$ and $y(k)$ are transformed to the two-dimensional frequency-warped signals $\bar{u}(k,\kappa)$ and $\bar{y}(k,\kappa)$, before being filtered by the warped PEF $\hat{A}(q,t)$ to obtain $\breve{u}[k, \hat{\boldsymbol{\alpha}}(t)]$ and $\breve{y}[k, \hat{\boldsymbol{\alpha}}(t)]$. By organizing the calculations in this way, none of the filtering operations involve an infinite number of filter states. An efficient algorithm for estimating the WLP model coefficients in $\boldsymbol{\alpha}(t)$ can be found in Härmä and Laine [35]: first the warped autocorrelation coefficients are calculated, which are then fed to a Levinson–Durbin recursion to find the model coefficient estimates.

5.3. PZLP near-end tonal components model

The PZLP PEF $A(q,t)/B(q,t)$ also has an infinite impulse response but, in contrast with the WLP PEF, an exact recursive computation is not possible in the PZLP case. Therefore, in all prefiltering operations involving the PZLP PEF, the initial denominator filter states are approximated by signal values that are prefiltered with an earlier estimate of the PZLP PEF denominator $B(q,t)$. The resulting algorithm is shown in Table 4. The PZLP approximations appear in steps 4 and 6a of Table 4, more specifically in the data matrices multiplying the PZLP PEF denominator coefficient vector $\hat{\mathbf{b}}(t) \triangleq [\hat{b}_1(t), \ldots, \hat{b}_{n_A}(t)]$ (which has been truncated such that the leading coefficient $\hat{b}_0(t) \equiv 1$ is

Table 3
PEM-based AFC algorithm: WLP near-end tonal components model.

for t
if $j = t \bmod P = 0$

(1) $d[k, \hat{\mathbf{f}}(t-1)] = y(k) - [u(k) \ \ldots \ u(k-n_F)]\hat{\mathbf{f}}(t-1), \quad k \in [t+P-M-n_C, t+P-1]$

(2) $$\mathbf{w}[t, \hat{\gamma}(t-P), \hat{\mathbf{f}}(t-1)] = \begin{bmatrix} d[t+P-M, \hat{\mathbf{f}}(t-1)] & \ldots & d[t+P-M-n_C, \hat{\mathbf{f}}(t-1)] \\ \vdots & \ddots & \vdots \\ d[t+P-1, \hat{\mathbf{f}}(t-1)] & \ldots & d[t+P-1-n_C, \hat{\mathbf{f}}(t-1)] \end{bmatrix} \hat{\mathbf{c}}(t-P)$$

(3) $\{\hat{\boldsymbol{\alpha}}(t), \sigma_A^2(t)\} = \mathrm{wlp}\{\mathbf{w}[t, \hat{\gamma}(t-P), \hat{\mathbf{f}}(t-1)]\}$

(4)
$$\begin{cases} \bar{u}(k,\kappa) = D_0^{-1}(q,\lambda) D^{\kappa}(q,\lambda) u(k), & k \in [t, t+P-1], \ \kappa \in [0, n_\alpha] \\ \bar{y}(k,\kappa) = D_0^{-1}(q,\lambda) D^{\kappa}(q,\lambda) y(k), & k \in [t, t+P-1], \ \kappa \in [0, n_\alpha] \\ \breve{u}[k, \hat{\boldsymbol{\alpha}}(t)] = \bar{u}(k,0) + [\bar{u}(k,1) \ \ldots \ \bar{u}(k,n_\alpha)]\hat{\boldsymbol{\alpha}}(t), & k \in [t+P-M-n_F, t+P-1] \\ \breve{y}[k, \hat{\boldsymbol{\alpha}}(t)] = \bar{y}(k,0) + [\bar{y}(k,1) \ \ldots \ \bar{y}(k,n_\alpha)]\hat{\boldsymbol{\alpha}}(t), & k \in [t+P-M, t+P-1] \\ \mathbf{r}[t, \hat{\boldsymbol{\alpha}}(t), \hat{\mathbf{f}}(t-1)] = \begin{bmatrix} \breve{y}[t+P-M, \hat{\boldsymbol{\alpha}}(t)] \\ \vdots \\ \breve{y}[t+P-1, \hat{\boldsymbol{\alpha}}(t)] \end{bmatrix} - \begin{bmatrix} \breve{u}[t+P-M, \hat{\boldsymbol{\alpha}}(t)] & \ldots & \breve{u}[t+P-M-n_F, \hat{\boldsymbol{\alpha}}(t)] \\ \vdots & \ddots & \vdots \\ \breve{u}[t+P-1, \hat{\boldsymbol{\alpha}}(t)] & \ldots & \breve{u}[t+P-1-n_F, \hat{\boldsymbol{\alpha}}(t)] \end{bmatrix} \hat{\mathbf{f}}(t-1) \end{cases}$$

(5) $\{\hat{\gamma}(t), \sigma_C^2(t)\} = \mathrm{lp}\{\mathbf{r}[t, \hat{\boldsymbol{\alpha}}(t), \hat{\mathbf{f}}(t-1)]\}$

(6a)
$$\begin{cases} \varepsilon[t, \hat{\boldsymbol{\alpha}}(t), \hat{\gamma}(t), \hat{\mathbf{f}}(t-1)] = \begin{bmatrix} r[t, \hat{\boldsymbol{\alpha}}(t), \hat{\mathbf{f}}(t-1)] & \ldots & r[t-n_C, \hat{\boldsymbol{\alpha}}(t), \hat{\mathbf{f}}(t-1)] \end{bmatrix} \hat{\mathbf{c}}(t) \\ \tilde{\mathbf{u}}[t, \hat{\boldsymbol{\alpha}}(t), \hat{\gamma}(t)] = \begin{bmatrix} \tilde{u}[t, \hat{\boldsymbol{\alpha}}(t), \hat{\gamma}(t)] \\ \vdots \\ \tilde{u}[t-n_F, \hat{\boldsymbol{\alpha}}(t), \hat{\gamma}(t)] \end{bmatrix} = \begin{bmatrix} \breve{u}[t, \hat{\boldsymbol{\alpha}}(t)] & \ldots & \breve{u}[t-n_C, \hat{\boldsymbol{\alpha}}(t)] \\ \vdots & \ddots & \vdots \\ \breve{u}[t-n_F, \hat{\boldsymbol{\alpha}}(t)] & \ldots & \breve{u}[t-n_F-n_C, \hat{\boldsymbol{\alpha}}(t)] \end{bmatrix} \hat{\mathbf{c}}(t) \end{cases}$$

else
(6b) as in Table 2
end if
(7)–(9) as in Table 2
end for

Table 4
PEM-based AFC algorithm: PZLP near-end tonal components model.

for t
if $j = t \bmod P = 0$

(1) $d[k, \hat{\mathbf{f}}(t-1)] = y(k) - [u(k) \ \dots \ u(k-n_F)]\hat{\mathbf{f}}(t-1), \quad k \in [t+P-M-\max(n_A, n_C), t+P-1]$

(2) $$\mathbf{w}[t, \hat{\gamma}(t-P), \hat{\mathbf{f}}(t-1)] = \begin{bmatrix} d[t+P-M, \hat{\mathbf{f}}(t-1)] & \dots & d[t+P-M-n_C, \hat{\mathbf{f}}(t-1)] \\ \vdots & \ddots & \vdots \\ d[t+P-1, \hat{\mathbf{f}}(t-1)] & \dots & d[t+P-1-n_C, \hat{\mathbf{f}}(t-1)] \end{bmatrix} \hat{\mathbf{c}}(t-P)$$

(3) $\{\hat{\boldsymbol{\alpha}}(t), \sigma_A^2(t)\} = \mathrm{pzlp}\{\mathbf{w}[t, \hat{\gamma}(t-P), \hat{\mathbf{f}}(t-1)]\}$

(4) $$\mathbf{r}[t, \hat{\boldsymbol{\alpha}}(t), \hat{\mathbf{f}}(t-1)] = \begin{bmatrix} d[t+P-M, \hat{\mathbf{f}}(t-1)] & \dots & d[t+P-M-n_A, \hat{\mathbf{f}}(t-1)] \\ \vdots & \ddots & \vdots \\ d[t+P-1, \hat{\mathbf{f}}(t-1)] & \dots & d[t+P-1-n_A, \hat{\mathbf{f}}(t-1)] \end{bmatrix} \hat{\mathbf{a}}(t)$$
$$- \begin{bmatrix} r[t+P-M-1, \hat{\boldsymbol{\alpha}}(t-P), \hat{\mathbf{f}}(t-1)] & \dots & r[t+P-M-n_A, \hat{\boldsymbol{\alpha}}(t-P), \hat{\mathbf{f}}(t-1)] \\ r[t+P-M, \hat{\boldsymbol{\alpha}}(t), \hat{\mathbf{f}}(t-1)] & \dots & r[t+P-M-n_A+1, \hat{\boldsymbol{\alpha}}(t-P), \hat{\mathbf{f}}(t-1)] \\ \vdots & \ddots & \vdots \\ r[t+P-2, \hat{\boldsymbol{\alpha}}(t), \hat{\mathbf{f}}(t-1)] & \dots & r[t+P-1-n_A, \hat{\boldsymbol{\alpha}}(t), \hat{\mathbf{f}}(t-1)] \end{bmatrix} \hat{\tilde{\mathbf{b}}}(t)$$

(5) $\{\hat{\gamma}(t), \sigma_C^2(t)\} = \mathrm{lp}\{\mathbf{r}[t, \hat{\boldsymbol{\alpha}}(t), \hat{\mathbf{f}}(t-1)])\}$

(6a)
$$\varepsilon[t, \hat{\boldsymbol{\alpha}}(t), \hat{\gamma}(t), \hat{\mathbf{f}}(t-1)] = \begin{bmatrix} r[t, \hat{\boldsymbol{\alpha}}(t), \hat{\mathbf{f}}(t-1)] & \dots & r[t-n_C, \hat{\boldsymbol{\alpha}}(t), \hat{\mathbf{f}}(t-1)] \end{bmatrix} \hat{\mathbf{c}}(t)$$
$$\begin{bmatrix} \breve{u}[t-n_F-n_C, \hat{\boldsymbol{\alpha}}(t)] \\ \vdots \\ \breve{u}[t+P-1, \hat{\boldsymbol{\alpha}}(t)] \end{bmatrix} = \begin{bmatrix} u(t-n_F-n_C) & \dots & u(t-n_F-n_C-n_A) \\ \vdots & \ddots & \vdots \\ u(t+P-1) & \dots & u(t+P-1-n_A) \end{bmatrix} \hat{\mathbf{a}}(t)$$
$$- \begin{bmatrix} \breve{u}[t-n_F-n_C-1, \hat{\boldsymbol{\alpha}}(t-P)] & \dots & \breve{u}[t-n_F-n_C-n_A, \hat{\boldsymbol{\alpha}}(t-P)] \\ \breve{u}[t-n_F-n_C, \hat{\boldsymbol{\alpha}}(t)] & \dots & \breve{u}[t-n_F-n_C-n_A+1, \hat{\boldsymbol{\alpha}}(t-P)] \\ \vdots & \ddots & \vdots \\ \breve{u}[t+P-2, \hat{\boldsymbol{\alpha}}(t)] & \dots & \breve{u}[t+P-1-n_A, \hat{\boldsymbol{\alpha}}(t)] \end{bmatrix} \hat{\tilde{\mathbf{b}}}(t)$$
$$\begin{bmatrix} \breve{y}[t-n_C+1, \hat{\boldsymbol{\alpha}}(t)] \\ \vdots \\ \breve{y}[t+P-1, \hat{\boldsymbol{\alpha}}(t)] \end{bmatrix} = \begin{bmatrix} y(t-n_C+1) & \dots & u(t-n_C+1-n_A) \\ \vdots & \ddots & \vdots \\ y(t+P-1) & \dots & y(t+P-1-n_A) \end{bmatrix} \hat{\mathbf{a}}(t)$$
$$- \begin{bmatrix} \breve{y}[t-n_C, \hat{\boldsymbol{\alpha}}(t-P)] & \dots & \breve{y}[t-n_C+1-n_A, \hat{\boldsymbol{\alpha}}(t-P)] \\ \breve{y}[t-n_C+1, \hat{\boldsymbol{\alpha}}(t)] & \dots & \breve{y}[t-n_C+2-n_A, \hat{\boldsymbol{\alpha}}(t-P)] \\ \vdots & \ddots & \vdots \\ \breve{y}[t+P-2, \hat{\boldsymbol{\alpha}}(t)] & \dots & \breve{y}[t+P-1-n_A, \hat{\boldsymbol{\alpha}}(t)] \end{bmatrix} \hat{\tilde{\mathbf{b}}}(t)$$
$$\tilde{\mathbf{u}}[t, \hat{\boldsymbol{\alpha}}(t), \hat{\gamma}(t)] = \begin{bmatrix} \tilde{u}[t, \hat{\boldsymbol{\alpha}}(t), \hat{\gamma}(t)] \\ \vdots \\ \tilde{u}[t-n_F, \hat{\boldsymbol{\alpha}}(t), \hat{\gamma}(t)] \end{bmatrix} = \begin{bmatrix} \tilde{u}[t, \hat{\boldsymbol{\alpha}}(t)] & \dots & \tilde{u}[t-n_C, \hat{\boldsymbol{\alpha}}(t)] \\ \vdots & \ddots & \vdots \\ \breve{u}[t-n_F, \hat{\boldsymbol{\alpha}}(t)] & \dots & \breve{u}[t-n_F-n_C, \hat{\boldsymbol{\alpha}}(t)] \end{bmatrix} \hat{\mathbf{c}}(t)$$

else
(6b) as in Table 2
end if
(7)–(9) as in Table 2
end for

lacking). The signal values in the upper triangular part (above and including the diagonal) of these matrices are prefiltered using the previously estimated PZLP PEF $\hat{A}(q, t-P)/\hat{B}(q, t-P)$ instead of using the current estimate. We should also remark that the matrix equations involving prefiltering with the PZLP PEF in steps 4 and 6a of Table 4 should be evaluated in a row-by-row fashion, since some of the output signal values needed in the right-hand side of the equation are only available in the precedings rows on the left-hand side.

The PZLP model coefficients can be estimated using the so-called constrained pole-zero linear prediction (CPZLP) method [44,45]. This method is similar to the adaptive notch filtering (ANF) method [46–48]; however, it operates iteratively on a batch of data instead of recursively updating the estimates of the PZLP model parameters. The main advantage of the batch estimation lies in the fact that the gradient estimates are recalculated using the entire data window in each iteration, which makes the algorithm less sensitive to the choice of the initial conditions as compared to the ANF algorithms [45].

6. Computational complexity and model approximations

6.1. Computational complexity

The computational complexity of the PEM-based AFC algorithms with cascaded near-end signal models can be quantified in terms of the average number of multiplications that have to be performed in each recursion. This complexity measure is shown in Table 5 for the three different near-end tonal components models, and also for the existing PEM-AFROW [21] and NLMS [24,

Table 5
Complexity comparison: average number of multiplications per recursion.

	(1)	(2)	(3)
NLMS	0	0	0
PEM-AFROW	$\frac{M}{P}(n_F+1)$	0	0
H_1 = PLP	$\frac{M+\max(n_A,n_C)}{P}(n_F+1)$	$\frac{M}{P}n_C$	$-\frac{2}{P}n_I^2+\frac{4M\Delta_K-5\Sigma_K+6M}{2P}n_I+\frac{2(M+1)\Delta_K-5\Sigma_K+6M+38}{2P}$
H_1 = WLP	$\frac{M+n_C}{P}(n_F+1)$	$\frac{M}{P}n_C$	$\frac{1}{P}n_\alpha^2+\frac{2M+4}{P}n_\alpha+\frac{M}{P}$
H_1 = PZLP	$\frac{M+\max(n_A,n_C)}{P}(n_F+1)$	$\frac{M}{P}n_C$	$\frac{\bar{\kappa}[(13+3\bar{\beta})M+(17+5\bar{\beta})]}{2P}n_A$

	(4)	(5)
NLMS	0	0
PEM-AFROW	0	$\frac{1}{P}n_C^2+\frac{M+4}{P}n_C+\frac{M}{P}$
H_1 = PLP	$\frac{M}{P}(n_I+3)$	$\frac{1}{P}n_C^2+\frac{M+4}{P}n_C+\frac{M}{P}$
H_1 = WLP	$\frac{M+n_\alpha}{P}(n_F+1)+\frac{2(M+P)-1}{P}n_\alpha+4$	$\frac{1}{P}n_C^2+\frac{M+4}{P}n_C+\frac{M}{P}$
H_1 = PZLP	$\frac{2M}{P}n_A$	$\frac{1}{P}n_C^2+\frac{M+4}{P}n_C+\frac{M}{P}$

	(6)	(7)	(8)	(9)
NLMS	n_F+1	0	$2(n_F+2)$	n_F+1
PEM-AFROW	$\frac{P+n_C}{P}(n_F+1)+\frac{2P-1}{P}n_C$	4	$2(n_F+2)$	n_F+1
H_1 = PLP	$\frac{P+n_I+n_C+2}{P}(n_F+1)+\frac{2}{P}(n_I+3)n_C+\frac{2(P-1)}{P}(n_I+n_C+3)$	4	$2(n_F+2)$	n_F+1
H_1 = WLP	$\frac{P+n_C-1}{P}(n_F+1)+2n_C$	4	$2(n_F+2)$	n_F+1
H_1 = PZLP	$\frac{P+2n_A+n_C-1}{P}(n_F+1)+\frac{4}{P}n_An_C+\frac{2(P-1)}{P}(2n_A+n_C)$	4	$2(n_F+2)$	n_F+1

Chapter 9] algorithms. The complexity measure has been calculated individually for each of the nine steps in the algorithm, such that the expressions in Table 5 can be easily compared with the corresponding descriptions given in Tables 2–4.

Before interpreting the expressions in Table 5, we should define the variables that have not appeared earlier: the fractional 3-tap pitch prediction method for estimating the PLP model coefficients requires the specification of limits $K_{\min}$ and $K_{\max}$ for the pitch lag K, and its computational complexity depends on the related quantities $\Delta_K \triangleq K_{\max}-K_{\min}$ and $\Sigma_K \triangleq K_{\max}+K_{\min}$, as well as on the order n_I of the fractional interpolation filter $I(q,l/D)$. The PZLP model coefficients are estimated using the CPZLP line search optimization algorithm, which requires on average $\bar{\beta}$ backtracking steps per iteration and $\bar{\kappa}$ iterations per parameter $\theta_i(t)$ in $\boldsymbol{\alpha}(t)$ [44].

The relative complexity of the different steps in the algorithm depends on the application area. In room acoustic applications, the required adaptive filter order n_F is typically much larger (i.e., several orders of magnitude) than the near-end signal model orders n_I, n_α, n_A, and n_C, and usually a few times larger than the data window length M and hop size P. As a consequence, the main extra complexity of the PEM-based algorithms in room acoustic applications is in steps 1 and 6, when compared to the NLMS complexity. Moreover, since the data window hop size P is often significantly larger than the near-end signal model orders, the complexity of step 6 comes close to the NLMS complexity of n_F+1 multiplications; hence the overall increase in complexity can almost completely be attributed to step 1 and approximately equals $2(n_F+1)$ multiplications (since we have suggested to choose $M=2P$), which is 50% of the overall NLMS complexity. Note that when the WLP near-end tonal components model is used, step 4 approximately involves another $2(n_F+1)$ multiplication such that the overall complexity is about twice the NLMS complexity. In HA applications, n_F is usually also larger than the near-end signal model orders n_I, n_α, n_A, and n_C, but similar to the squared near-end signal model orders n_I^2, n_α^2, n_A^2, and n_C^2 and the multiplied orders n_In_C, n_An_C, and $n_\alpha n_C$. Consequently, steps 3, 5, and 6 contribute more significantly to the overall complexity than in the room acoustic case. However, this contribution is negligible for $P \geq \{n_I, n_\alpha, n_A, n_C\}$. Finally, an important feature of the PEM-based algorithms is that no additional complexity is introduced in the adaptive filtering part of the algorithm (i.e., steps 7–9), so when using a more demanding adaptive filtering algorithm like the recursive least squares (RLS) or affine projection algorithm (APA), the extra complexity of the PEM-based algorithms does not increase accordingly.

6.2. Model approximations

In the PEM-based AFC algorithms, the data vectors that are needed for the identification of $\mathbf{f}(t)$, $\boldsymbol{\alpha}(t)$, and $\boldsymbol{\gamma}(t)$ are recalculated entirely once in every P recursions, see steps

1, 2, 4, and 6a in the algorithms given in Tables 2–4. These prefiltering operations may contribute significantly to the overall computational complexity, as can be seen from Table 5. However, by applying certain model approximations, the number of prefiltering operations can be reduced significantly without sacrificing too much of the AFC performance.

These model approximations are related to the stationarity of the acoustic feedback path $F(q,t)$ and the near-end signal models $H_1(q,t)$ and $H_2(q,t)$. If these models are assumed to be piecewise stationary with time scales of Q_F+1, $Q_{H_1}+1$, and $Q_{H_2}+1$ samples, respectively, then the corresponding model estimates $\hat{F}(q,t)$, $\hat{H}_1(q,t)$, and $\hat{H}_2(q,t)$ can be assumed equal on similar time scales, i.e.,

$$F(q,t-Q_F)=\cdots=F(q,t)$$
$$\Rightarrow \hat{F}(q,t-Q_F)=\cdots=\hat{F}(q,t) \quad (46)$$
$$H_1(q,t-Q_{H_1})=\cdots=H_1(q,t)$$
$$\Rightarrow \hat{H}_1(q,t-Q_{H_1})=\cdots=\hat{H}_1(q,t) \quad (47)$$
$$H_2(q,t-Q_{H_2})=\cdots=H_2(q,t)$$
$$\Rightarrow \hat{H}_2(q,t-Q_{H_2})=\cdots=\hat{H}_2(q,t) \quad (48)$$

Obviously, the above approximations are only exact if the time index t corresponds to the final time index of a stationarity time interval for $F(q,t)$, $H_1(q,t)$, and $H_2(q,t)$, and if the model estimates have zero variance. Nevertheless, we will apply (46)–(48) without explicitly assuming that these two conditions are fulfilled.

When applying the approximations in (46)–(48) to the algorithms given in Tables 2–4, we can apply the following simplifications:

- In step 1, we can approximate $\hat{\mathbf{f}}(t-1)$ by $\hat{\mathbf{f}}(k)$ for $k=t-Q_F-1,\ldots,t-2$ such that $d[k,\hat{\mathbf{f}}(t-1)]$ is approximated by $d[k,\hat{\mathbf{f}}(k)]$, which is the a posteriori feedback-compensated signal that has been calculated in step 9 of the kth recursion. This simplification leads to an average computational saving of $((n_F+1)/P)\min[Q_F,M-P+\max(n_A,n_C)]$ multiplications per recursion (or $((n_F+1)/P)\min(Q_F,M-P+n_C)$ multiplications in the WLP case).
- In step 2, we may replace $\hat{\mathbf{c}}(t-P)$ by $\hat{\mathbf{c}}(t-lP)$, $l=2,\ldots,\lfloor Q_{H_2}/P\rfloor+1$, such that only the first $M-(\lfloor Q_{H_2}/P\rfloor+1)P$ and the last P elements of the prefiltered data vector $\mathbf{w}[t,\hat{\boldsymbol{\gamma}}(t-P),\hat{\mathbf{f}}(t-1)]$ have to be recalculated using $\hat{\mathbf{c}}(t-P)$, while the other elements are copied and shifted from the previous data vector $\mathbf{w}[t-P,\hat{\boldsymbol{\gamma}}(t-2P),\hat{\mathbf{f}}(t-P-1)]$. In this way, an average number of $n_C\min(\lfloor Q_{H_2}/P\rfloor,(M-P)/P)$ multiplications per recursion can be saved.
- In step 4, a similar approximation $\hat{\mathbf{a}}(t)=\hat{\mathbf{a}}(t-lP)$, $l=1,\ldots,\lfloor Q_{H_1}/P\rfloor$ may again lead to a computational saving: on average $(n_I+3)\min(\lfloor Q_{H_1}/P\rfloor,(M-P)/P)$ multiplications per recursion in the PLP case and $2n_A\min(\lfloor Q_{H_1}/P\rfloor,(M-P)/P)$ in the PZLP case. In the WLP case, the calculation of $\check{u}[k,\hat{\boldsymbol{\alpha}}(t)]$ and $\check{y}[k,\hat{\boldsymbol{\alpha}}(t)]$ can be simplified in a similar way, saving on average $n_\alpha\min(\lfloor Q_{H_1}/P\rfloor,(M-P+n_F)/P)$ and $n_\alpha\min(\lfloor Q_{H_1}/P\rfloor,(M-P)/P)$ multiplications per recursion, respectively, while the computation of $\mathbf{r}[t,\hat{\boldsymbol{\alpha}}(t),\hat{\mathbf{f}}(t-1)]$ can be simplified using (46) to save on average $((n_F+1)/P)\min(Q_F,M-P)$ multiplications per recursion.
- In step 6a, the approximation $\hat{\mathbf{a}}(t)=\hat{\mathbf{a}}(t-lP)$, $l=1,\ldots,\lfloor Q_{H_1}/P\rfloor$ may yield a saving of $(n_I+3)[\min(\lfloor Q_{H_1}/P\rfloor,(n_F+n_C)/P)+\min(\lfloor Q_{H_1}/P\rfloor,(n_C-1)/P)]$ multiplications per recursion in the PLP case and $2n_A[\min(\lfloor Q_{H_1}/P\rfloor,(n_F+n_C)/P)+\min(\lfloor Q_{H_1}/P\rfloor,(n_C-1)/P)]$ in the PZLP case. Approximating $\hat{\mathbf{c}}(t)=\hat{\mathbf{c}}(t-lP)$, $l=1,\ldots,\lfloor Q_{H_2}/P\rfloor$ further leads to a saving of $n_C\min(\lfloor Q_{H_2}/P\rfloor,n_F/P)$ multiplications per recursion for all cases.

Since the data window size M should be chosen as large as possible without violating the assumption that the near-end signal models are stationary in the entire data window, we typically have $M\approx Q_{H_1}\approx Q_{H_2}$. The stationarity time scale of the acoustic feedback path depends heavily on the nature of the changes in the acoustic environment. In PA applications, variations in room acoustics are mainly due to microphone/loudspeaker movements, people moving around the room, and temperature variations. The time scale of room acoustic variations due to moving people (hence also due to objects being moved by people) has been estimated to be around 10 ms for wideband audio applications, while temperature variations are considerably slower [49]. In HA applications, the largest feedback path variations have been found to result from external effects (e.g., by using a telephone set or due to changes in the enclosing room acoustics) [50]; hence the variability time scale may be assumed similar to that found in PA applications. When using 50% overlapping data windows of 40–60 ms, e.g., $M=2P=2048$ at $f_s=44.1$ kHz, the main computational overhead of approximately $2(n_F+1)$ multiplications (due to step 1) can be reduced to $1.6(n_F+1)$ multiplications in fast changing environments ($Q_F=10\,\text{ms}\times 44.1\,\text{kHz}=441$), or n_F+1 multiplications in slowly changing environments ($Q\geq M-P+n_C\approx 1058=24\,\text{ms}\times 44.1\,\text{kHz}$). In this way, the additional complexity of the proposed PEM-based AFC algorithm compared to NLMS reduces to 25–40% of the overall NLMS complexity.

7. Simulation results

We will evaluate the performance of the proposed PEM-based AFC algorithms with cascaded near-end signal models by means of simulation results obtained in two substantially different scenarios. The first scenario is a typical PA scenario (at $f_s=44.1$ kHz), in which the sound of a single musical instrument is picked up by a microphone, amplified, and fed back from the loudspeaker to the microphone through a room acoustic feedback path. The second scenario is related to HA applications, by simulating a HA that processes an incoming classical music signal at $f_s=16$ kHz. We should emphasize that, except for the adaptive filter length n_F, identical values of all the algorithm parameters are used in both simulation scenarios. It can hence be understood that the algorithm parameters are not particularly optimized to provide a

good AFC performance in one specific simulation scenario, but instead are chosen such as to be generally applicable.

The algorithm parameters are chosen as follows: at $f_s = 44.1$ kHz, the data window length $M = 2048$ and the hop size $P = M/2 = 1024$, while at $f_s = 16$ kHz, $M = 1024$ and $P = M/2 = 512$. The near-end tonal components model order is chosen such as to be able to model 15 tonal components in each data window, i.e., $n_A = 30$ for the PZLP model, whereas $n_\alpha = 30$ for the WLP model. The near-end noise components model order is also set to $n_C = 30$. A processing delay of $d_1 = P - 1$ samples is inserted in the electro-acoustic forward path to allow $P - 1$ future data samples to be included in the LP data window. In this way, the identifiability condition in (40) is fulfilled without the need for inserting an additional processing delay d_2 in the adaptive filtering circuit. Moreover, the electro-acoustic forward path contains a hard clipping saturation function to avoid numerical overflow in case of system instability. The PLP model identification features a pitch lag range between $K_{\min} = \lfloor f_s/1000 \rfloor$ and $K_{\max} = \lfloor f_s/100 \rfloor$ corresponding to fundamental frequencies in the range 100–1000 Hz. The interpolation ratio for estimating fractional pitch lag values $K + l/D$ is set to $D = 8$, and the fractional interpolation filter order is chosen as $n_l = 31$. In the identification of the WLP near-end tonal components model, the warping parameter is chosen such that the warping map approximates the Bark scale as suggested in Smith and Abel [51]: $\lambda_{\text{Bark}}(f_s) = 1.0674\sqrt{(2/\pi)\arctan(0.06583 f_s)} - 0.1916$. The PZLP model is identified using the CPZLP algorithm parameters suggested in van Waterschoot and Moonen [44] and with an initial estimate of $\hat{\theta}_i^{(0)}(t) = (2\pi 440)/f_s$ for

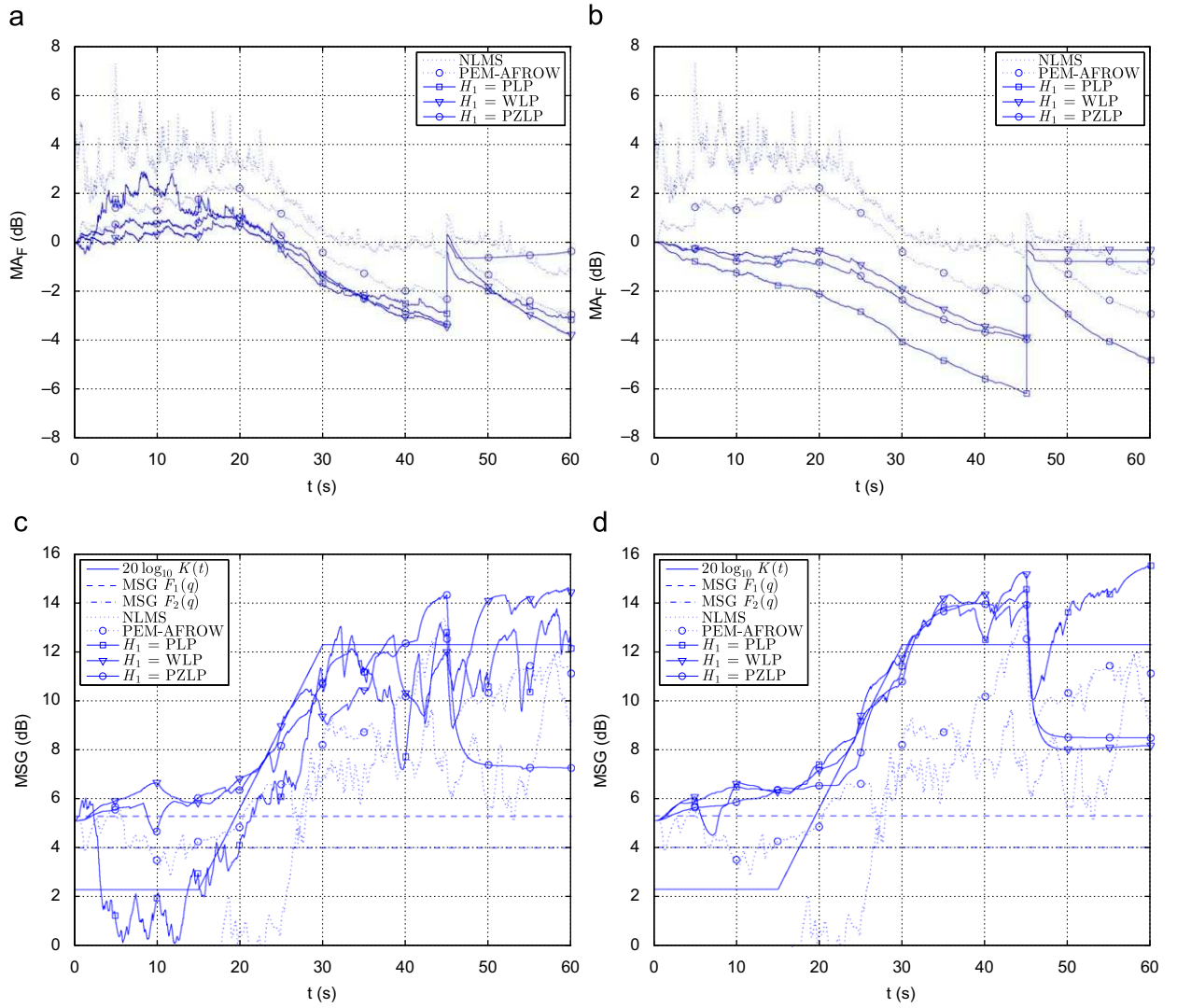

Fig. 3. Comparison of PEM-based AFC algorithm with NLMS and PEM-AFROW in a PA application: (a) misadjustment if only a near-end tonal components model $H_1(q,t)$ is used, (b) misadjustment if cascaded near-end models $H_1(q,t)$ and $H_2(q,t)$ are used, (c) MSG if only a near-end tonal components model $H_1(q,t)$ is used, (d) MSG if cascaded near-end models $H_1(q,t)$ and $H_2(q,t)$ are used.

all the PZLP model angles. The prediction error power $\sigma_\varepsilon^2(t)$ is estimated using an effective data window length of M samples by setting the forgetting factor $\lambda_\varepsilon = 1 - 1/M$. Finally, the stochastic gradient algorithm for updating the feedback path estimate features a step size $\mu = 0.005$ and a regularization parameter $\delta = 10^{-6}$. Unless mentioned otherwise, no model approximations are applied in the simulations, i.e., $Q_F = Q_{H_1} = Q_{H_2} = 0$.

Both simulation scenarios have a temporal layout made up of four phases of equal duration. During the first phase of the simulation, the electro-acoustic forward path broadband gain factor $K(t)$ is fixed to a value that would result in a 3 dB gain margin if no AFC algorithm were applied. In the second phase, the gain $20\log_{10} K(t)$ is increased linearly with time, until a value is attained that is 10 dB above the gain applied in the first phase. This simulated gain increase resembles the way an AFC algorithm is applied in practice, i.e., PA operators and HA users are expected to turn on the AFC algorithm at a relatively low gain value and subsequently raise the gain to benefit from the MSG increase provided by the AFC algorithm. Moreover, this gain increase leads to an improved AFC convergence, since the ratio of the feedback signal power to the near-end signal power is increased. In the third phase, the gain is fixed to the final gain value in the second phase, while the fourth phase features a simulated acoustic feedback path change.

In the PA simulation scenario, the near-end signal is a 60 s excerpt from the Partita No. 2 in D minor (Allemande) for solo violin by Bach [53]. The motivation for using a violin piece is that the violin appears to be a problematic instrument in terms of sound amplification in PA applications, which is probably due to its highly frequency-dependent directivity [52]. The acoustic feedback path

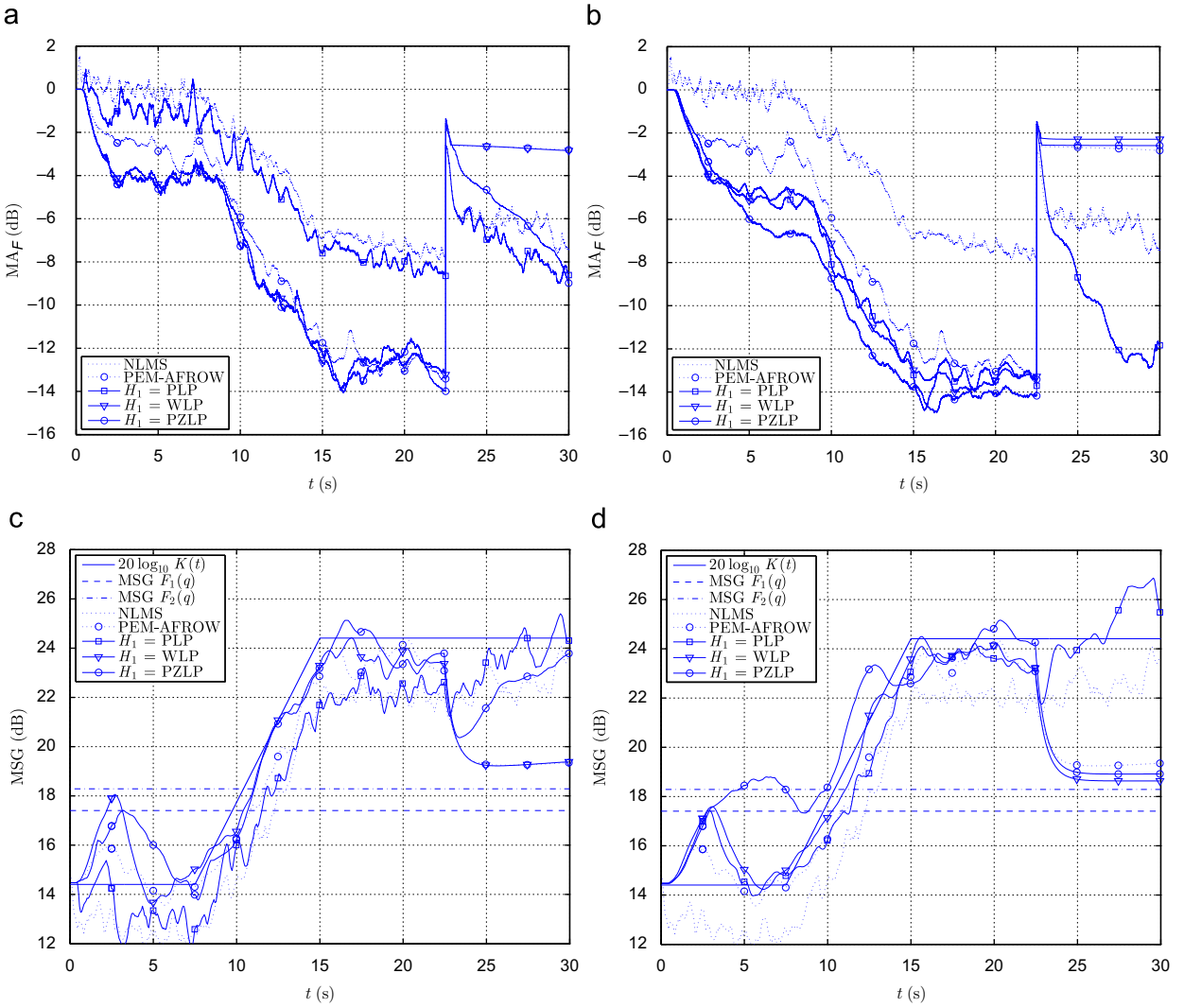

Fig. 4. Comparison of PEM-based AFC algorithm with NLMS and PEM-AFROW in a HA application: (a) misadjustment if only a near-end tonal components model $H_1(q,t)$ is used, (b) misadjustment if cascaded near-end models $H_1(q,t)$ and $H_2(q,t)$ are used, (c) MSG if only a near-end tonal components model $H_1(q,t)$ is used, (d) MSG if cascaded near-end models $H_1(q,t)$ and $H_2(q,t)$ are used.

impulse response has a length of 100 ms (corresponding to $n_F = 4410$ samples) and was measured in a medium-sized room. The AFC performance is quantified by evaluating the misadjustment, defined as

$$\mathrm{MA}_F(\mathrm{dB}) = 20\log_{10}\frac{\|\hat{\mathbf{f}}(t) - \mathbf{f}\|}{\|\mathbf{f}\|} \tag{49}$$

and the MSG defined in (11) as a function of time. The results when only a near-end tonal components model $H_1(q,t)$ is used (with $H_2(q,t) \equiv 1$) are shown in Figs. 3(a) and (c), while the results with cascaded near-end models are displayed in Figs. 3(b) and (d). In both cases, the NLMS [24, Chapter 6] and PEM-AFROW (with $n_C = 30$) [21] algorithm performance is also included for reference. It can be observed that by only including a near-end tonal components model, the AFC misadjustment as compared to the PEM-AFROW algorithm can be improved when using the PLP, WLP, and PZLP models. However, when using the cascaded near-end signal models, a much more significant performance improvement can be obtained, particularly when a PLP near-end tonal components model is applied. Some of the algorithms appear not to be able to cope with an acoustic feedback path change when operating at a high gain value, hence closed-loop instability results (apparent from the horizontal misadjustment curves in Figs. 3(a) and (b)). In terms of the MSG, the AFC algorithm should converge fast enough such that its MSG increases at least as fast as the gain factor $20\log_{10}K(t)$, otherwise ringing and howling effects will occur. The best MSG performance is obtained when the PLP, WLP, and PZLP near-end tonal components models are cascaded with a noise components model. In Figs. 3(c) and (d), the instantaneous gain value $20\log_{10}K(t)$, as well as the MSG values without AFC is also shown (with "MSG $F_1(q)$" and "MSG $F_2(q)$" denoting the MSG before and after the acoustic feedback path change). An MSG increase of more than 11 dB w.r.t. the case when no AFC is applied is obtained for the cascaded structure with a PLP tonal components model (compared to an 8 dB MSG increase with the PEM-AFROW algorithm).

The HA simulation reflects a scenario in which a HA user is listening to a musical recording or performance. In this simulation, the near-end signal is a 16 s excerpt from the first part (Kyrie) of the Mass in C minor ("Grosse Messe", K427) by Mozart [54], which features a soprano, chorus, and orchestra. The acoustic feedback path is a 12.5 ms measured HA feedback path impulse response, i.e., $n_F + 1 = 200$. The misadjustment and MSG curves are given in Figs. 4(a) and (c) for a near-end tonal components model only and in Figs. 4(b) and (d) for cascaded near-end signal models. In contrast to the PA scenario, the HA simulation results indicate that the existing PEM-based AFC algorithms such as PEM-AFROW may work fine in audio applications too, as was also observed in Spriet et al. [18,32]. This can be explained by the fact that the conventional LP model (which is used in these existing PEM-based AFC algorithms) is better suited for modeling audio signals at lower sampling frequencies [30]. However, the AFC performance may be further improved by using cascaded near-end signal models, particularly with a PZLP tonal components model, which clearly results in the fastest AFC convergence and MSG increase. However, the algorithm with the PZLP tonal components model appears to be non-robust to acoustic feedback path changes, hence the PLP tonal components model may be a better choice. The largest MSG increase compared to the MSG without AFC equals more than 8 dB, which is approximately 3 dB larger than the MSG increase obtained with the PEM-AFROW algorithm.

Finally, we evaluate the applicability of the model approximations introduced in Section 6.2. In Figs. 5(a) and (b), we show the misadjustment convergence curves for the PEM-based AFC algorithm with cascaded near-end signal models for five different combinations of values for Q_F, Q_{H_1}, and Q_{H_2}. Each of these variables is either set to zero, or to the value which delivers the maximum achievable computational saving. It can be seen that in the PA case (with a PLP tonal components model), a rather unexpected performance improvement occurs when Q_{H_1} and/or Q_{H_2} is increased. In the HA case (with a PZLP tonal

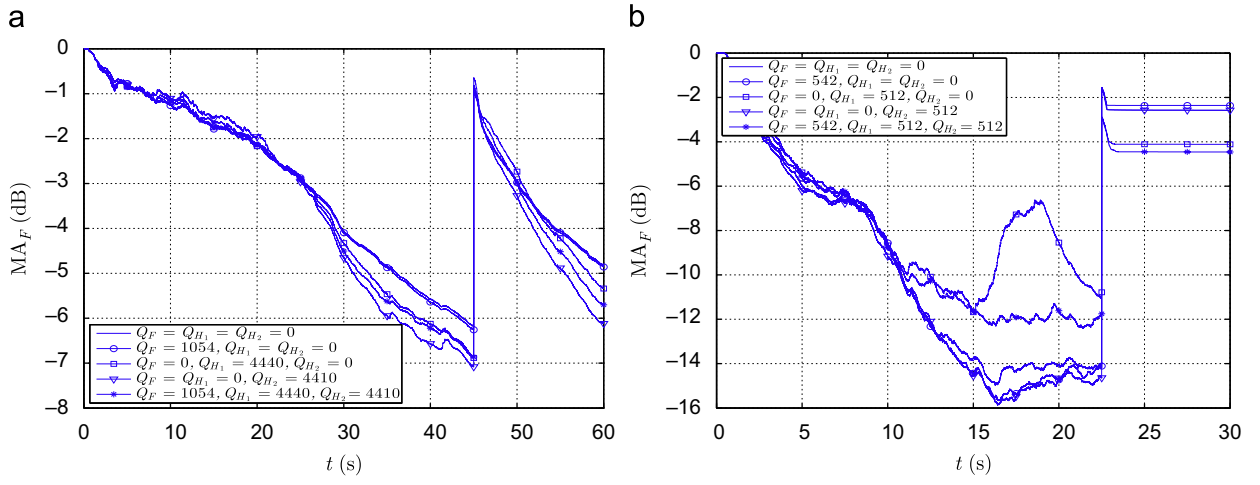

Fig. 5. Evaluation of model approximations in PEM-based AFC algorithm with cascaded near-end signal models: misadjustment for different stationarity time scales Q_F, Q_{H_1}, and Q_{H_2}, (a) PA application (with PLP tonal components model), (b) HA application (with PZLP tonal components model).

components model), increasing Q_{H_2} leads to a slightly better performance, while increasing Q_{H_2} may lead to a severe performance decrease.

8. Conclusion

In this paper, we have proposed a modification to the PEM-based AFC approach, which consists in replacing the all-pole near-end signal model by a cascade of two linear models. In this way, the PEM-based AFC approach, which was originally designed for speech applications only, can also be applied to audio applications involving musical sound signals. Since the cascaded near-end signal models are able to whiten the near-end signal component in the microphone signal more effectively, a significant AFC performance improvement is obtained. Three different algorithms have been presented, in which the organization of the prefiltering operations is specifically tailored to the underlying near-end tonal components model structure. The computational requirements of these algorithms were analyzed in detail, leading to the conclusion that a complexity increase of 50% of the overall NLMS complexity can be expected. However, if model approximations related to the stationarity of the feedback path and the near-end signal are applied, the computational overhead can further be reduced to 25% of the NLMS complexity without significantly influencing the AFC performance. Both in PA and in HA simulation scenarios, a considerable improvement in the acoustic feedback path misadjustment and the MSG has been observed. In particular, the PZLP and PLP near-end tonal components models, which both feature a PEF that behaves as a cascade of notch filters, have been found to offer the best performance.

Acknowledgements

This research work was carried out at the ESAT Laboratory of Katholieke Universiteit Leuven, in the frame of K.U. Leuven Research Council CoE EF/05/006 Optimization in Engineering (OPTEC), the Belgian Programme on Interuniversity Attraction Poles initiated by the Belgian Federal Science Policy Office IUAP P6/04 (DYSCO, 'Dynamical systems, control and optimization', 2007–2011), and the Concerted Research Action GOA-AMBioRICS, and was supported by the Institute for the Promotion of Innovation through Science and Technology in Flanders (IWT-Vlaanderen). The scientific responsibility is assumed by its authors.

References

[1] T. van Waterschoot, M. Moonen, 50 years of acoustic feedback control: state of the art and future challenges, in: Proceedings of IEEE, ESAT-SISTA Technical Report TR 08-13, Katholieke Universiteit Leuven, Belgium, February 2009 (Online). Available from: ⟨ftp://ftp.esat.kuleuven.be/pub/sista/vanwaterschoot/abstracts/08-13.html⟩, submitted for publication.

[2] M.P. Lewis, T.J. Tucker, D.M. Oster, Method and apparatus for adaptive audio resonant frequency filtering, U.S. Patent 5,245,665, September 1993.

[3] M. Börsch, Method for constraining electroacoustic feedback, European Patent Application EP1684543 A1, July 2006.

[4] N. Osmanovic, V.E. Clarke, E. Velandia, An in-flight low latency acoustic feedback cancellation algorithm, in: Preprints AES 123rd Convention, New York, NY, USA, 2007, AES Preprint 7266.

[5] T. van Waterschoot, M. Moonen, Comparative evaluation of howling detection criteria in notch-filter-based howling suppression, in: Preprints AES 126th Convention, Munich, Germany, 2009, AES Preprint 7752.

[6] D.K. Bustamante, T.L. Worrall, M.J. Williamson, Measurement and adaptive suppression of acoustic feedback in hearing aids, in: Proceedings of 1989 IEEE International Conference on Acoustics, Speech, and Signal Processing (ICASSP '89), vol. 3, Glasgow, UK, 1989, pp. 2017–2020.

[7] J.M. Kates, Feedback cancellation in hearing aids: results from a computer simulation, IEEE Trans. Signal Process. 39 (3) (1991) 553–562.

[8] H.A.L. Joson, F. Asano, Y. Suzuki, T. Sone, Adaptive feedback cancellation with frequency compression for hearing aids, J. Acoust. Soc. Amer. 94 (6) (1993) 3248–3254.

[9] J.A. Maxwell, P.M. Zurek, Reducing acoustic feedback in hearing aids, IEEE Trans. Speech Audio Process. 3 (4) (1995) 304–313.

[10] C.P. Janse, P.A.A. Timmermans, Signal amplifier system with improved echo cancellation, U.S. Patent 5,748,751, May 1998.

[11] S. Kamerling, K. Janse, F. van der Meulen, A new way of acoustic feedback suppression, in: Preprints AES 104th Convention, Amsterdam, The Netherlands, 1998, AES Preprint 4735.

[12] M.G. Siqueira, A. Alwan, Steady-state analysis of continuous adaptation in acoustic feedback reduction systems for hearing-aids, IEEE Trans. Speech Audio Process. 8 (4) (2000) 443–453.

[13] J. Hellgren, U. Forssell, Bias of feedback cancellation algorithms in hearing aids based on direct closed loop identification, IEEE Trans. Speech Audio Process. 9 (7) (2001) 906–913.

[14] J. Hellgren, Analysis of feedback cancellation in hearing aids with filtered-X LMS and the direct method of closed-loop identification, IEEE Trans. Speech Audio Process. 10 (2) (2002) 119–131.

[15] C.P. Janse, C.C. Tchang, Acoustic feedback suppression, WIPO Patent Application WO/2005/079109, August 2005.

[16] A. Ortega, E. Lleida, E. Masgrau, L. Buera, A. Miguel, Acoustic feedback cancellation in speech reinforcement systems for vehicles, in: Proceedings of Interspeech 2005, Lisbon, Portugal, 2005, pp. 2061–2064.

[17] A. Ortega, E. Lleida, E. Masgrau, Speech reinforcement system for car cabin communications, IEEE Trans. Speech Audio Process. 13 (5) (2005) 917–929.

[18] A. Spriet, I. Proudler, M. Moonen, J. Wouters, Adaptive feedback cancellation in hearing aids with linear prediction of the desired signal, IEEE Trans. Signal Process. 53 (10) (2005) 3749–3763.

[19] N.A. Shusina, B. Rafaely, Unbiased adaptive feedback cancellation in hearing aids by closed-loop identification, IEEE Trans. Audio Speech Lang. Process. 14 (2) (2006) 658–665.

[20] G. Schmidt, T. Haulick, Signal processing for in-car communication systems, Signal Process. 86 (6) (2006) 1307–1326 (special issue on Applied Speech and Audio Processing).

[21] G. Rombouts, T. van Waterschoot, K. Struyve, M. Moonen, Acoustic feedback suppression for long acoustic paths using a nonstationary source model, IEEE Trans. Signal Process. 54 (9) (2006) 3426–3434.

[22] C. Boukis, D.P. Mandic, A.G. Constantinides, Towards bias minimization in acoustic feedback cancellation systems, J. Acoust. Soc. Amer. 121 (3) (2007) 1529–1537.

[23] G. Rombouts, T. van Waterschoot, M. Moonen, Robust and efficient implementation of the PEM-AFROW algorithm for acoustic feedback cancellation, J. Audio Eng. Soc. 55 (11) (2007) 955–966.

[24] S. Haykin, Adaptive Filter Theory, Prentice-Hall, Englewood Cliffs, NJ, 1996.

[25] L. Ljung, T. Söderström, Theory and Practice of Recursive Identification, MIT Press, Cambridge, MA, 1986.

[26] L. Ljung, System Identification: Theory for the User, Prentice-Hall, Englewood Cliffs, NJ, 1987.

[27] T. van Waterschoot, G. Rombouts, P. Verhoeve, M. Moonen, Double-talk-robust prediction error identification algorithms for acoustic echo cancellation, IEEE Trans. Signal Process. 55 (3) (2007) 846–858.

[28] S.M. Kay, The effects of noise on the autoregressive spectral estimator, IEEE Trans. Acoust. Speech Signal Process. ASSP-27 (5) (1979) 478–485.

[29] Y.T. Chan, J.M.M. Lavoie, J.B. Plant, A parameter estimation approach to estimation of frequencies of sinusoids, IEEE Trans. Acoust. Speech Signal Process. ASSP-29 (2) (1981) 214–219.

[30] T. van Waterschoot, M. Moonen, Comparison of linear prediction models for audio signals, EURASIP J. Audio Speech Music Process (2008), 24. Article ID 706935, doi:10.1155/2008/706935.
[31] H. Nyquist, Regeneration theory, Bell Syst. Tech. J. 11 (1932) 126–147.
[32] A. Spriet, K. Eneman, M. Moonen, J. Wouters, Objective measures for real-time evaluation of adaptive feedback cancellation algorithms in hearing aids, in: Proceedings of 16th European Signal Processing Conference (EUSIPCO '08), Lausanne, Switzerland, 2008.
[33] G. Rombouts, T. van Waterschoot, K. Struyve, P. Verhoeve, M. Moonen, Identification of undermodelled room impulse responses, in: Proceedings of 2005 International Workshop Acoustic Echo Noise Control (IWAENC '05), Eindhoven, The Netherlands, 2005, pp. 153–156.
[34] U. Forssell, L. Ljung, Closed-loop identification revisited, Automatica 35 (7) (1999) 1215–1241.
[35] A. Härmä, U.K. Laine, A comparison of warped and conventional linear predictive coding, IEEE Trans. Speech Audio Process. 9 (5) (2001) 579–588.
[36] T. van Waterschoot, Design and evaluation of digital signal processing algorithms for acoustic feedback and echo cancellation, Ph.D. Thesis, Katholieke Universiteit Leuven, Leuven, Belgium, March 2009 (Online). Available from: ⟨http://hdl.handle.net/1979/2599⟩.
[37] T. van Waterschoot, G. Rombouts, M. Moonen, Dually regularized recursive prediction error identification for acoustic feedback and echo cancellation, in: Proceedings of 15th European Signal Processing Conference (EUSIPCO '07), Poznań, Poland, 2007, pp. 1610–1614.
[38] M.A. Stone, B.C.J. Moore, Tolerable hearing aid delays. I. Estimation of limits imposed by the auditory path alone using simulated hearing losses, Ear Hearing 20 (3) (1999) 182–191.
[39] J. Makhoul, Linear prediction: a tutorial review, Proc. IEEE 63 (4) (1975) 561–578.
[40] P. Kroon, B.S. Atal, Pitch predictors with high temporal resolution, in: Proceedings of 1990 IEEE International Conference on Acoustics, Speech, and Signal Processing (ICASSP '90), vol. 2, Albuquerque, NM, USA, 1990, pp. 661–664.
[41] Y. Qian, G. Chahine, P. Kabal, Pseudo-multi-tap pitch filters in a low bit-rate CELP speech coder, Speech Commun. 14 (4) (1994) 339–358.
[42] R.P. Ramachandran, P. Kabal, Pitch prediction filters in speech coding, IEEE Trans. Acoust. Speech Signal Process. ASSP-37 (4) (1989) 467–478.
[43] T. van Waterschoot, M. Moonen, Adaptive feedback cancellation for audio signals using a warped all-pole near-end signal model, in: Proceedings of 2008 IEEE International Conference on Acoustics, Speech, and Signal Processing (ICASSP '08), Las Vegas, NV, USA, 2008, pp. 269–272.
[44] T. van Waterschoot, M. Moonen, Constrained pole-zero linear prediction: an efficient and near-optimal method for multi-tone frequency estimation, in: Proceedings of 16th European Signal Processing Conference (EUSIPCO '08), Lausanne, Switzerland, 2008.
[45] T. van Waterschoot, M. Diehl, M. Moonen, Constrained pole-zero linear prediction: optimization of cascaded biquadratic notch filters for multi-tone and multi-pitch estimation, ESAT-SISTA Technical Report TR 07-115, Katholieke Universiteit Leuven, Belgium, February 2008.
[46] A. Nehorai, A minimal parameter adaptive notch filter with constrained poles and zeros, IEEE Trans. Acoust. Speech Signal Process. ASSP-33 (4) (1985) 983–996.
[47] M.V. Dragošević, S.S. Stanković, An adaptive notch filter with improved tracking properties, IEEE Trans. Signal Process. 43 (9) (1995) 2068–2078.
[48] G. Li, A stable and efficient adaptive notch filter for direct frequency estimation, IEEE Trans. Signal Process. 45 (8) (1997) 2001–2009.
[49] L.M. van de Kerkhof, W.J.W. Kitzen, Tracking of a time-varying acoustic impulse response by an adaptive filter, IEEE Trans. Signal Process. 40 (6) (1992) 1285–1294.
[50] J. Hellgren, T. Lunner, S. Arlinger, Variations in the feedback of hearing aids, J. Acoust. Soc. Amer. 106 (5) (1999) 2821–2833.
[51] J.O. Smith, J.S. Abel, Bark and ERB bilinear transforms, IEEE Trans. Speech Audio Process. 7 (6) (1999) 697–708.
[52] H.J. Vos, O. Warusfel, N. Misdariis, D. de Vries, Analysis and reproduction of the frequency spectrum and directivity of a violin, J. Acoust. Soc. Neth. (167) (2003).
[53] J.S. Bach, Partita for solo violin No. 2 in D minor, BWV 1004 (Allemande), Mark Lubotsky, violin, Brilliant Classics, 99701/11, 1987.
[54] W.A. Mozart, Mass No. 17 for soloists, chorus, and orchestra in C minor (“Grosse Messe”), K427 (Kyrie), Philippe Herreweghe, Conductor, Harmonia Mundi, 801393, 1991.